KTH Chemical Science
and Engineering

TAILORING SURFACE PROPERTIES OF BIO-FIBERS VIA ATOM TRANSFER RADICAL POLYMERIZATION

Josefina Lindqvist

AKADEMISK AVHANDLING

Som med tillstånd av Kungliga Tekniska Högskolan i Stockholm framlägges till offentlig granskning för avläggande av teknisk doktorsexamen fredagen den 20 april 2007, kl 10.00 i sal D3, Lindstedtsvägen 5, KTH, Stockholm. Avhandlingen försvaras på engelska.

TRITA-CHE-Report 2007:16
ISSN 1654-1081
ISBN 978-91-7178-616-6

ABSTRACT

The potential use of renewable, bio-based polymers in high-technological applications has attracted great interest due to increased environmental concern. Cellulose is the most abundant biopolymer resource in the world, and it has great potential to be modified to suit new application areas. The development of controlled polymerization techniques, such as atom transfer radical polymerization (ATRP), has made it possible to graft well-defined polymers from cellulose surfaces. In this study, graft-modification of cellulose substrates by ATRP was explored as a tool for tailoring surface properties and for the fabrication of functional cellulose surfaces.

Various native and regenerated cellulose substrates were successfully graft-modified to investigate the effect of surface morphology on the grafting reactions. It was found that significantly denser polymer brushes were grafted from the native than from the regenerated cellulose substrates, most likely due to differences in surface area.

A method for detaching the grafted polymer from the substrate was developed, based on the selective cleavage of silyl ether bonds with tetrabutylammonium fluoride. The results from the performed kinetic study suggest that the surface-initiated polymerization of methyl methacrylate from cellulose proceeds faster than the concurrent solution polymerization at low monomer conversions, but slows down to match the kinetics of the solution polymerization at higher conversions.

Superhydrophobic and self-cleaning bio-fiber surfaces were obtained by grafting of glycidyl methacrylate using a branched graft-on-graft architecture, followed by post-functionalization to obtain fluorinated polymer brushes. AFM analysis showed that the surface had a micro-nano-binary structure. It was also found that superhydrophobic surfaces could be achieved by post-functionalization with an alkyl chain, with no use of fluorine.

Thermo-responsive cellulose surfaces have been prepared by graft-modification with the stimuli responsive polymer poly(*N*-isopropylacrylamide) (PNIPAAm). Brushes of poly(4-vinylpyridine) (P4VP) rendered a pH-responsive cellulose surface. Dual-responsive cellulose surfaces were achieved by grafting block-copolymers of PNIPAAm and P4VP.

SAMMANFATTNING

Den potentiella användningen av förnyelsebara, biobaserade polymerer i högteknologiska tillämpningar har tilldragit sig stort intresse på grund av ökad miljömedvetenhet. Cellulosa är den rikligast förekommande biopolymerresursen i världen, och den har stor potential att kunna modifieras för att passa nya tillämpningsområden. Utvecklandet av kontrollerade polymerisationstekniker, såsom atom transfer radical polymerization (ATRP), har gjort det möjligt att ympa väldefinierade polymerer från cellulosaytor. I den här studien har ympmodifiering av cellulosasubstrat via ATRP utforskats som ett verktyg för att skräddarsy ytegenskaper, samt för framställandet av funktionella cellulosaytor.

Olika slags naturliga och regenererade cellulosasubstrat ympmodifierades för att undersöka effekten av ytmorfologi på ympreaktionerna. Det framgick att signifikant tätare polymerborst kunde ympas från de naturliga, jämfört med de regenererade cellulosaytorna, troligtvis på grund av skillnader i ytarea.

En metod för att avskilja den ympade polymeren från substratet utvecklades, baserad på den selektiva klyvningen av silyleterbindningar med tetrabutylammoniumfluorid. Resultaten från den genomförda kinetikstudien talar för att den ytinitierade polymerisationen av metylmetakrylat från cellulosa sker snabbare än den jämlöpande lösningspolymerisationen vid låga monomeromsättningar, men saktar ner till att bli jämförbar med polymerisationen i lösningen vid högre omsättningar.

Superhydrofoba och självrengörande biofiberytor erhölls genom ympning av glycidylmetakrylat under användande av en grenad ymp-på-ymp-arkitektur, följd av post-funktionalisering för att erhålla fluorinerade polymerborst. AFM-analys visade att ytan hade en mikro-nano-binär struktur. Det framgick även att superhydrofoba ytor kunde framställas genom post-funktionalisering med en alkylkedja, utan användning av fluor.

Termoresponsiva cellulosaytor har framställts genom ympmodifiering med den stimuliresponsiva polymeren poly(*N*-isopropylakrylamid) (PNIPAAm). Borst av poly(4-vinylpyridin) (P4VP) frambringade en pH-responsiv cellulosayta. Dubbelresponsiva cellulosaytor framställdes genom ympning av block-sampolymerer av PNIPAAm och P4VP.

LIST OF PAPERS

The thesis is a summary of the following papers:

I. "Surface Modification of Natural Substrates by Atom Transfer Radical Polymerization", J. Lindqvist, E. Malmström, *Journal of Applied Polymer Science*, **2006**, *100*, 4155-4162

II. "Kinetic Study of the Surface-Initiated Atom Transfer Radical Polymerization from Bio-Fiber Surfaces", J. Lindqvist, D. Nyström, A. Hult, E. Malmström, *Macromolecules*, submitted

III. "Superhydrophobic Bio-Fibre Surfaces *via* Tailored Grafting Architecture", D. Nyström, J. Lindqvist, E. Östmark, A. Hult, E. Malmström, *Chemical Communications*, **2006**, 3594-3595

IV. "Superhydrophobic and Self-Cleaning Bio-Fibre surfaces via ATRP and subsequent post-functionalisation", D. Nyström, J. Lindqvist, E. Östmark, P. Antoni, M. Johansson, E. Malmström, A. Hult, *Soft Matter*, submitted

V. "Dual-Responsive Bio-Fiber Surfaces *via* ATRP", J. Lindqvist, D. Nyström, E. Östmark, P. Antoni, M. Johansson, A. Hult, E. Malmström, *Macromolecules*, submitted

The contribution of the author of this thesis to the appended papers is:

I. All the experimental work and preparation of the manuscript.

II. A majority of the experimental work, and most of the preparation of the manuscript.

III, V. About half of the experimental work and preparation of the manuscript. Involved in all parts of the work.

IV. Some parts of the experimental work and preparation of the manuscript. Took part in outlining the experimental work, and in the evaluation of the results.

TABLE OF CONTENTS

1 PURPOSE OF THE STUDY

The interest in using cellulose in high-technological products is constantly increasing. Cellulose is the most abundant renewable polymer resource in the world, and it has the potential to be modified to further improve its properties. The development of controlled radical polymerization techniques has made it possible to graft well-defined polymers from a cellulose-based surface, in order to tailor the surface properties for specific functions. The ability to create functional cellulose surfaces opens up for a new range of possible applications for bio-based materials as sensors, membranes, in electronics and biomedical applications.

This study was conducted to explore the use of atom transfer radical polymerization (ATRP) of vinyl monomers as a versatile tool to tailor the surface properties of bio-fibers and to investigate how the surface-initiated polymerization is affected by the morphology of the cellulose-based substrate. In order to achieve this, various cellulose-based substrates had to be investigated and compared. To fully characterize and understand the surface-initiated polymerizations from cellulose, it was necessary to develop a method to cleave the polymer brushes from the substrate. The following aim was to explore the ability to achieve functional cellulose surfaces using ATRP.

2 INTRODUCTION

2.1 CONTROLLED RADICAL POLYMERIZATION

Free radical polymerization is the most widely used industrial polymerization method. The advantages over other techniques are primarily the low requirements on reactant purity, and the wide range of monomers that can be used. The main drawback is, however, the lack of control over molecular weight, molecular weight distribution and chain end-groups. Over the last fifteen years the development of controlled radical polymerization techniques has opened up for achieving well-defined polymer structures and functionalities using vinyl monomers. The three most studied controlled radical polymerization techniques are nitroxide mediated polymerization (NMP),[1] atom transfer radical polymerization (ATRP)[2-4] and reversible addition-fragmentation chain transfer (RAFT) polymerization.[5,6] These methods are all based on suppressing termination and other unwanted side-reactions by maintaining a low concentration of active propagating species. This is accomplished by establishing a dynamic equilibrium between active species and end-capped (dormant) chains which are unable to propagate or terminate (Scheme 1). The exchange between active and dormant species should be fast relative to propagation, and the equilibrium should be shifted towards the dormant species.

Scheme 1. General CRP equilibrium between active and dormant species.

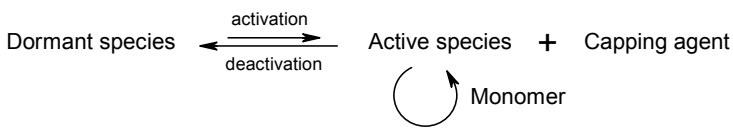

2.1.1 Atom transfer radical polymerization (ATRP)

ATRP was first reported independently by Wang and Matyjaszewski[2,3] and Sawamoto and coworkers[4] in 1995, and has since then been the most studied of the controlled radical polymerization techniques. It was derived from atom

transfer radical addition (ATRA), initially developed by Kharasch.[7] ATRA involves atom transfer of a halogen atom from an organic halide to a metal complex, followed by addition of the formed organic radical to an alkene, and finally back-transfer of the halogen atom. In ATRP, the addition product is able to re-activate into a radical and undergo propagation with available monomer as an equilibrium is established between the dormant halogen capped chains and the active radical species. A successful ATRP has a small proportion of terminated chains, and a uniform chain growth which is accomplished by a fast and quantitative initiation and rapid reversible deactivation.[8]

The ATRP system is composed of monomer, initiator and a catalyst consisting of a transition metal halide complexed with a ligand. A variety of monomers, such as styrenes,[2,9] (meth)acrylates,[2,10-15] (meth)acrylamides[16,17] and acrylonitrile[18,19] can be utilized and the choice of monomer determines the type of initiator and catalyst that can be employed.[20] The initiator is usually an alkyl halide, typically a bromide or chloride. The initiation should proceed faster than, or at least equal to the propagation, why the reactivity of the initiator towards the monomer must be at least comparable to that of the growing polymer chain. The initiators are therefore often chosen to match the structure of the polymer analogue.[8] The catalyst is an important component of the ATRP system as it determines the dynamics of the equilibrium between dormant and active species. The most frequently studied transition metal is copper, due to its synthetic versatility and low cost. However, ATRP has also been successfully mediated by a number of other metals, including iron,[21-23] ruthenium,[4,24] osmium,[25] molybdenum,[26-28] rhenium,[29] nickel,[30,31] palladium,[32] rhodium,[33,34] cobalt[35] and titanium.[36] A wide variety of mostly nitrogen-,[3,10,37-39] but also phospine-based[4,21,22,24] ligands has been used to complex the transition metal.

ATRP can be conducted in a range of solvents, such as toluene, diphenyl ether, ethyl acetate, acetone, methanol, water and supercritical carbon dioxide.[8] Aqueous ATRP has received significant attention, due to increased environmental concern and also the possible biomedical applications for hydrophilic polymers.[11,12,40-47]

The main drawback of ATRP is the relatively large amount of catalyst used, which needs to be removed from the final polymer. To overcome this problem, methods to decrease the amount of catalyst in the system, and to remove the catalyst in the final polymer, have been investigated.[47,48]

2.1.1.1 Mechanism and kinetics of ATRP

The mechanism of copper-mediated ATRP, adapted from that of ATRA as proposed by Matyjazewski *et al.*,[49] is shown in Scheme 2. It involves initiation by homolytic cleavage of an alkyl halide bond by a copper halide complex to

generate the corresponding higher oxidation state copper halide complex and an alkyl radical. The active radical species can then propagate with available monomer, or be deactivated by back-transfer of the halogen in the reversible redox reaction. The rate of deactivation must be higher than the rate of activation to suppress termination reactions and thus ensure a controlled polymerization. In the initial stages of the polymerization, equal amounts of active species and Cu(II) are formed during the activation, and the rates of activation and deactivation are similar. Termination by radical recombination then occurs at this stage, as the rate of termination is higher than the rate of deactivation. However, for every termination reaction, the concentration of Cu(II) increases, shifting the equilibrium gradually to the dormant side of the reaction, resulting in a lower rate of polymerization and less termination. This self-adjustment of the system is known as the persistent radical effect.[50]

Scheme 2. Mechanism of copper-mediated ATRP.

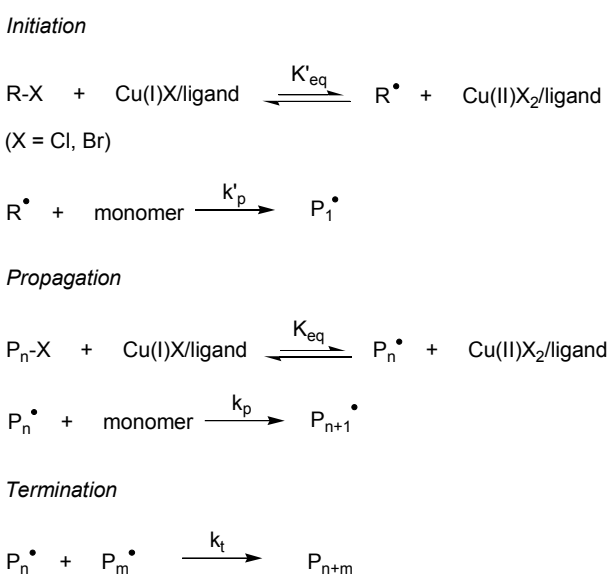

From the reactions in Scheme 2, using the assumption that termination can be neglected due to the persistent radical effect and a fast pre-equilibrium approximation, the kinetics of ATRP can be described by the following equations:[49]

$$K_{eq} = \frac{k_{act}}{k_{deact}} = \frac{[P^{\bullet}][Cu(II)X_2]}{[Cu(I)X][PX]} \quad (1)$$

$$R_p = k_{app}[M] = k_p[P^{\bullet}][M] = k_p K_{eq}[RX]\frac{[Cu(I)X]}{[Cu(II)X_2]}[M] \quad (2)$$

In equation 2, the propagation rate (R_p) is described as first-order in respect to monomer concentration [M], initiator concentration [RX] and activator concentration [Cu(I)X], and negatively first order in respect to deactivator concentration [Cu(II)X_2]. However, since the concentration of Cu(II)X_2 increases with occurring termination reactions due to the persistent radical effect, the actual kinetics may be more complex.[8,50]

It has been shown that the rate of polymerization is accelerated in polar solvents.[42,45,51] This has led to the proposal of other theories on the polymerization mechanism of ATRP. Haddleton and co-workers suggested that the active propagating species is a caged radical, associated to the metal complex, rather than a free radical.[52] More recently, Percec *et al.* suggested that the copper-mediated polymerization in polar solvents, and with most commonly used ligands, proceeds *via* a single electron transfer mechanism rather than atom transfer, as the Cu(I)X dissociates into Cu(0) and Cu(II) in these solvents, where after the Cu(0) mediates the activation of the dormant chain *via* an ion cage intermediate.[53]

2.2 POLYMER BRUSHES

Modification of surfaces with covalently linked polymer films can be used to tailor the surface properties of solid substrates. The modification can be conducted by attaching polymers by one end to the surface, yielding polymer brushes.[54] This can be performed either by physisorption of the polymer or by covalent attachment. The latter of these two methods is preferred as it renders the brushes more thermally and solvolytically stable.[55] Covalently bound polymer brushes can be achieved by 'grafting to' or 'grafting from' techniques. The 'grafting to' method involves attachment of pre-synthesized, end-functionalized polymer chains to reactive groups on the surface (Figure 1). The polymers can be fully characterized before the attachment to the surface, offering the possibility to control the properties of the resulting material. However, steric hindrance for the attachment increases during the reaction as the polymer chains have to diffuse through the layer of already attached brushes to reach the reactive sites on the surface. Thus, it is very difficult to achieve high grafting densities using the 'grafting to' method.[55] In the 'grafting from' technique, the

polymer brushes are formed by *in situ* surface-initiated polymerization from immobilized initiators on the substrate (Figure 2). Using this method, it is possible to obtain thicker polymer films and higher grafting densities.[55] In order to tailor the properties of the grafts, it is highly desirable to use of a controlled technique to conduct the surface-initiated polymerization. Over the last years, all the major controlled polymerization techniques have been used to fabricate polymer brushes. Of these, ATRP has become the most popular route due to its compatibility with a wide range of functional monomers, and the experimental accessibility compared to other techniques.

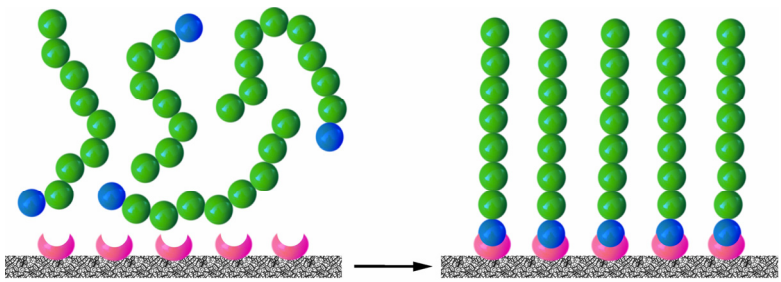

Figure 1. Schematic representation of the 'grafting-to' technique.

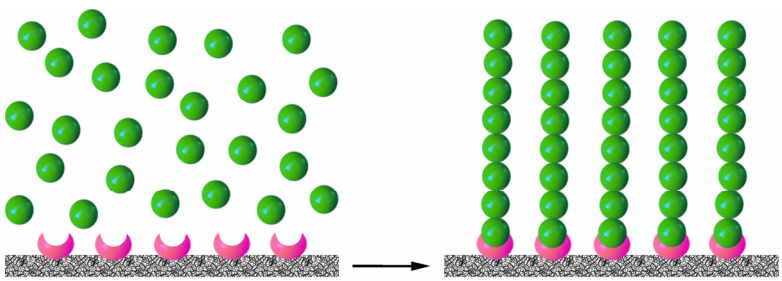

Figure 2. Schematic representation of the 'grafting-from' technique.

2.2.1 Surface-initiated ATRP

Surface-initiated ATRP has proven to be a versatile technique for the fabrication of well-defined polymer brushes from a variety of solid substrates.[56-65] ATRP offers the possibility to further tailor the properties of the brushes by grafting of block-copolymers from the surface, as first reported by Matyjaszewski and coworkers.[59]

The surface-initiated ATRP from smooth, planar substrates is, however, complicated by the low concentration of initiator in the system, yielding a very

small amount of Cu(II) species formed after the halogen transfer. The amount may be too low to effectively deactivate the propagating radicals, causing uncontrolled chain-growth.[66] To overcome this challenge, deactivating Cu(II) halide can be added to the system in the beginning of the reaction to effectively shift the equilibrium to the dormant side.[59] An additional method to control the surface-initiated polymerization is to add a free 'sacrificial' initiator to the system, allowing sufficient concentrations of the deactivating Cu(II) species to be generated via the initial termination of radicals formed in the solution.[56,57] The sacrificial initiator, however, yields free polymer which is necessary to separate from the grafted polymer, resulting in a tedious work-up process. On the other hand, the free polymer can be analyzed by conventional techniques, and the length of the brushes can be tailored by adjusting the monomer-to-free initiator ratio. However, pre-determination of the brush length assumes that the kinetics of the surface-initiated polymerization and the solution polymerization is similar. In order to study this, and to fully characterize the grafted polymer brushes it is necessary to cleave them from the surface.[67] Comparison of free and cleaved polymer showing similar kinetics has been reported by Fukuda *et al.*, using a porous glass filter[68] and silica particles[69] as substrate, and by Fontaine *et al.* using Wang resin.[70]

2.2.2 Functional surfaces

The ability to fabricate well-defined polymer brushes with controlled properties has led to the increasing interest in producing functional surfaces, such as superhydrophobic[71], antibacterial,[72] non-fouling,[73] and stimuli responsive[74] materials. These kind of materials have potential use in a wide variety of applications, including microfluidic devices, sensors, actuators, drug delivery, and bioseparation.[75-77] Two groups of functional surfaces that have been widely studied over the last years are superhydrophobic and stimuli responsive surfaces.

2.2.2.1 Superhydrophobic surfaces

Superhydrophobic surfaces have attracted increasing interest over the last years due to their water repellency, self-cleaning and anti-fouling properties that will offer potential use in various applications.[78-80] The hydrophobicity can be characterized by depositing a water droplet on the surface and measuring the water contact angle, which is the angle between the solid-water and water-air interfaces. For a flat solid surface, the contact angle (θ) can be described with Young's equation:

$$\cos\theta = \frac{\gamma_{sv} - \gamma_{sl}}{\gamma_{lv}} \quad (3)$$

where γ is the surface tension of the solid-vapor (sv), solid-liquid (sl), and liquid-vapor (lv) interfaces, respectively.

However, both the surface chemistry and the roughness affect the hydrophobicity of the material. The contact angle for a rough surface (θ^*) can be described with different modifications of Young's equation developed by Wenzel[81] and Cassie and Baxter.[82]

In the Wenzel state, the water droplet is in contact with the entire surface area, making the droplet stick to the surface (Figure 3a). This results in a high hysteresis (the difference between advancing and receding contact angle). The surface roughness (r) is the ratio of the actual contact area to the apparent surface area, and the contact angle for the rough surface can be described in terms of the Young contact angle as:

$$\cos\theta^* = r\cos\theta \quad (4)$$

In the Cassie-Baxter state, the water droplet does not penetrate into the cavities on the surface, but instead rests on top of these, thus creating air pockets (Figure 3b). The contact angle θ^* can then be described as:

$$\cos\theta^* = \phi_s \cos\theta + \phi_s - 1 \quad (5)$$

where ϕ_s is the fraction of the area under the water droplet that is in contact with water. The Cassie-Baxter state has a low hysteresis and sliding angle (the tilt angle at which a water droplet on a surface starts to move), as the water droplet can roll off easily when it rests on air pockets. This state is therefore necessary for self-cleaning applications.

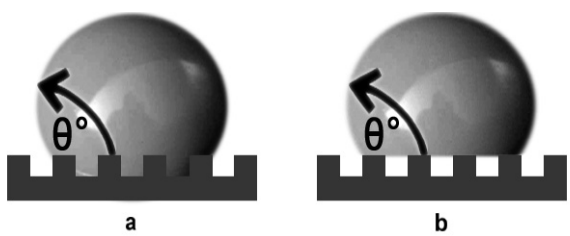

Figure 3. Effects of roughness on hydrophobicity according to a) Wenzel and b) Cassie and Baxter.

Superhydrophobic surfaces should exhibit water contact angles higher than 150° in combination with low sliding angles.[83,84] These kind of surfaces cannot be produced only by lowering the surface free energy of a flat surface, without adding the effect of surface roughness. The most well-known example of a superhydrophobic material in nature is the Lotus leaf, where a hydrophobic waxy material is combined with a binary structure of micro- and nano-sized texture.[85] Synthetic superhydrophobic surfaces are usually fabricated by increasing the roughness of a hydrophobic material, or by modifying a rough substrate with hydrophobic compounds.[80,86-93]

2.2.2.2 Stimuli-responsive surfaces

Stimuli-responsive surfaces change properties upon an external trigger, such as temperature, pH, electric field, radiation or ionic strength.[94,95] The reversible switch in surface properties can be used for selective adhesion/detachment, controlled uptake and release, and transduction of chemical energy into mechanical work.[75,76] Stimuli-responsive surfaces can be accomplished by graft-modification with a stimuli-responsive polymer.[75,96] The grafted polymer brush will then reversibly change its conformation in contact with the external stimuli.

A widely studied thermo-responsive polymer is poly(*N*-isopropylacrylamide) (PNIPAAm) which exhibits a lower critical solution temperature (LCST) around 32 °C.[97,98] PNIPAAm is water soluble below LCST, due to hydrogen-bonding between the polymer chains and water molecules. At temperatures above LCST, intramolecular hydrogen-bonding results in a water insoluble polymer.[99] Thus, PNIPAAm brushes grafted from a surface changes conformation from extended hydrophilic below LCST to collapsed hydrophobic at temperatures above LCST, causing the wettability of the surface to change from hydrophilic to hydrophobic (Figure 4).[74,100-107] Furthermore, PNIPAAm-

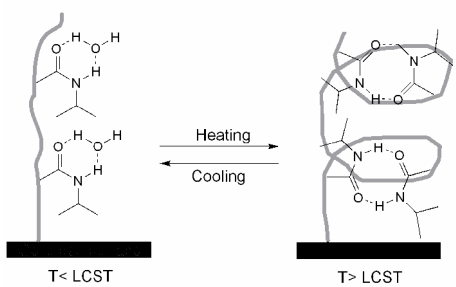

Figure 4. Conformation of PNIPAAm brushes below (left), and above (right) LSCT.

modified surfaces have proven useful for controlling cell adhesion and detachment by the switch in wettability.[74,108-110]

To produce surfaces that respond to variations in pH, poly(acrylic acid) (PAA) or poly(4-vinylpyridine) (P4VP) can be grafted from the substrate. A PAA-grafted surface is hydrophobic with collapsed polymer brushes below pH 4, and becomes hydrophilic at higher pH values as the PAA chains assume an extended conformation due to deprotonation of the acid groups.[111] P4VP, on the other hand, is water soluble below pH 5, due to protonation of the pyridyl groups, and water insoluble in the deprotonated state.[112] Brittain and co-workers prepared a pH-responsive silicon surface by graft-modification of block-copolymers comprising of PAA and P4VP.[113] Copolymer brushes with different kinds of responsive polymers allow adjustable surface properties using multiple external triggers. Jiang and co-workers reported on the fabrication of a dual-responsive silicon surface by grafting copolymers of PAA and PNIPAAm.[114]

2.3 CELLULOSE

Cellulose is the most abundant biopolymer in the world. It is the main component of the cell wall in a majority of the higher plants, but is also produced by certain bacteria, algae and fungi.[115] Cellulose is a linear polysaccharide made up of β-D-glucopyranose units liked together by (1→4)-glycosidic bonds (Figure 5). Every second glucopyranose unit is rotated 180°, why the repeating unit of cellulose, cellobiose, is considered to be a dimer of glucopyranose units.[115] The

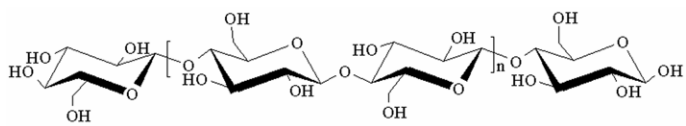

Figure 5. Structure of cellulose.

many hydroxyl groups and the linear structure of cellulose result in the formation of intra- and intermolecular hydrogen bonding, causing the cellulose chains to aggregate into three-dimensional, highly crystalline structures.[115] Cellulose exists in different crystalline forms, the most common known as cellulose I-IV. Cellulose I is the native form of cellulose, in which the crystal structure consists of parallel cellulose chains.[116] If the cellulose is treated with strong base (mercerization) or regenerated by dissolution and recrystallization, the crystal structure is converted into cellulose II. This crystal structure has antiparallel chains and is more thermodynamically stable than cellulose I.[117]

2.3.1 Bio-fibers

A plant fiber is mainly built up by cellulose, hemicelluloses and lignin. The cellulose molecules form sheets, held together by hydrogen bonds, which stack together to form highly crystalline microfibrils.[117] The microfibrils form bundles to make up the fibrils, which in turn build up the different layers of the fiber wall together with hemicelluloses and lignin. The orientation of the fibrils differs between the different layers of the cell wall, improving the mechanical properties of the fiber.[117] A schematic structure of a wood fiber can be seen in Figure 6.

The fibers are extracted from wood by different pulping techniques. During chemical pulping, much of the lignin and hemicelluloses are removed, resulting in a more compact fiber structure. Fibers from some other plants, such as cotton, naturally have higher cellulose content than wood.[115]

Natural cellulose fibers find use in many important applications due to their useful properties, such as a high modulus combined with low specific weight.

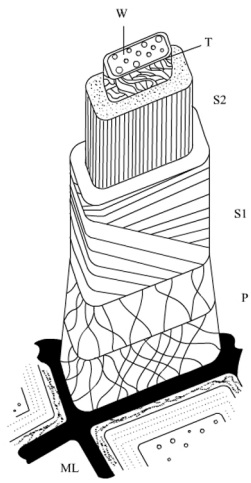

Figure 6. Schematic structure of a wood fiber.

2.3.2 Graft-modification of cellulose

Cellulose is already used in a wide variety of applications, and the interest in expanding the field of possible applications is constantly increasing. Due to its many hydroxyl groups, cellulose is, however, very hydrophilic and adsorbs water easily. This complicates the use of cellulose in applications such as reinforcing agent in composites where adhesion to the often hydrophobic

polymer matrix is necessary. On the other hand, the hydroxyl groups can also serve as reactive sites, providing the cellulose with great potential for modification to improve and/or tailor the properties to a certain function. Surface modification of cellulose by graft-copolymerization provides an important method for altering chemical and physical properties.[118] Grafting of a hydrophobic polymer to cellulose fibers can for example provide the increased hydrophobicity needed to solve the adhesion problem for the use in composites.[119,120] Graft-modification of cellulose has been widely studied for several decades.[118,121-132] Various techniques have been employed, most of them based on the 'grafting from' method where radicals are generated along the cellulose backbone, followed by conventional free radical polymerization of vinyl monomers. Grafting of cellulose *via* controlled polymerization techniques has been accomplished using the 'grafting to' method, usually by pre-forming the polymers *via* anionic or cationic polymerization, followed by coupling to the cellulose backbone.[133-135] Daly *et al.* reported the first controlled grafting from cellulose *via* NMP.[136] Grafting from cellulose has since then also been achieved *via* ATRP[64] and RAFT.[137] The use of ATRP to graft-copolymerize cellulose has made it possible to accurately tailor properties such as wettability[138] and antimicrobial activity.[139]

3 EXPERIMENTAL

The following section briefly describes the performed experimental procedures. Full details can be found in the appended papers.

3.1 MATERIALS

Native cellulose (cellulose I) substrates were used in planar form in terms of Whatman 1 filter paper, and as a powder in terms of microcrystalline cellulose (MCC, Aldrich). Regenerated cellulose substrates were used in planar form in terms of dialysis membrane (Spectra/Por®3, MWCO 3500), and as fibers in terms of Lyocell (kindly supplied by Professor Lars Wågberg, manufactured by Lenzing). Chitosan films were used as a planar polysaccharide substrate (kindly supplied by Dr. Mikael Gällstedt at STFI-Packforsk).

Methyl acrylate (MA, 99%, Aldrich), methyl methacrylate (MMA, 99%, Aldrich), styrene (99%, Acros) and glycidyl methacrylate (GMA, 97%, Acros) were passed through a column of neutral aluminum oxide prior to use. 4-Vinylpyridine (4VP, 95%, Aldrich) was passed through a column of basic aluminum oxide prior to use. N-isopropylacrylamide (NIPAAm, 97%, Aldrich) was recrystallized twice from hexane. Tris(2-(dimethylamino)ethyl)amine (Me_6-TREN) was prepared similar to the procedure by Ciampolini and Nardi[140] from tris(2-aminoethyl)amine (98% Aldrich). All other chemicals and solvents were used as received.

3.2 CHARACTERIZATION

Infrared spectra were recorded on a Perkin-Elmer Spectrum 2000 FT-IR equipped with a MKII Golden Gate, Single Reflection ATR System from Specac Ltd, London, U.K. The ATR crystal was a MKII heated Diamond 45 ° ATR Top Plate.

Size Exclusion Chromatography (SEC) using THF (1.0 mL min^{-1}) as the mobile phase was performed at 35 °C using a Viscotek TDA model 301 equipped with two GMH_{HR}-M columns with TSK-gel (mixed bed, MW resolving range: 300-100 000) from Tosoh Biosep, a VE 5200 GPC autosampler, a VE 1121 GPC solvent pump, and a VE 5710 GPC degasser (all from Viscotek corp.). A universal calibration method was created using broad and narrow linear polystyrenes

standards. Corrections for the flow rate fluctuations were made using THF as an internal standard. Viscotek Trisec 2000 version 1.0.2 software was used to process data. A conventional calibration method was created using narrow linear polystyrenes standards. Corrections for the flow rate fluctuations were made using toluene as an internal standard. Viscotek OmniSEC version 4.0 software was used to process data.

^{1}H NMR spectra were recorded on a Bruker Avance 400 MHz NMR instrument using $CDCl_3$ as solvent. The solvent residual signal was used as internal standard.

Static water contact angles were measured with a Rame-Hart goniometer using MilliQ water at ambient temperature and humidity. Static and dynamic contact angle measurements were also conducted on a KSV instruments CAM 200 equipped with a Basler A602f camera, using 5 μL droplets of MilliQ water or pH buffer. The contact angles were determined using the CAM software.

Scanning Electron Microscopy (SEM) was conducted on a JEOL JSM-5400. The samples were sputtered with Au/Cd (60%/40%) in a Desk II from Denton Vacuum.

Imaging of the surfaces was performed in tapping-mode on a NanoScope IIIa Multimode AFM, using silicon tips (supplied by Veeco) with resonance frequencies of 303-344 kHz (according to the manufacturer).

3.3 SURFACE MODIFICATION OF BIO-FIBERS

3.3.1 Immobilization of initiator on cellulose surface

To enable the grafting reaction, the hydroxyl groups on the surface of the substrates were first esterified by reaction with 2-bromoisobutyryl bromide or 2-chloroproionyl chloride, yielding covalently bound ATRP initiators on the surface as shown in Scheme 3. The procedure for immobilization of initiator on the surface was adopted from Carlmark and Malmström.[138] The cellulose substrates were washed and ultrasonicated in tetrahydrofuran and acetone prior

Scheme 3. Immobilization of initiator on cellulose.

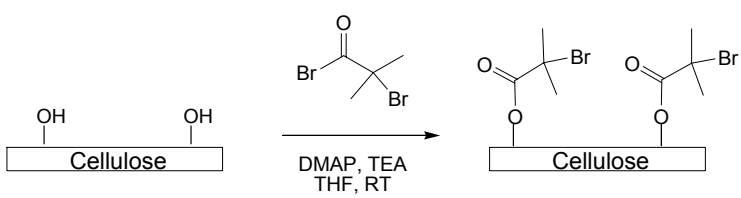

to the modification. The hydroxyl groups on the surface were then reacted by immersing the substrate in a solution containing 2-bromoisobuturyl bromide or 2-chloropropionyl chloride, triethylamine (TEA) and a catalytic amount of 4-dimethyl aminopyridine (DMAP) in tetrahydrofuran (THF). The reaction was allowed to proceed at room temperature for 4-24 h. The substrates were thereafter thoroughly washed with THF and ethanol and dried in a vacuum oven at 50 °C.

Scheme 4. Silane-functionalization, and subsequent immobilization of initiator on cellulose.

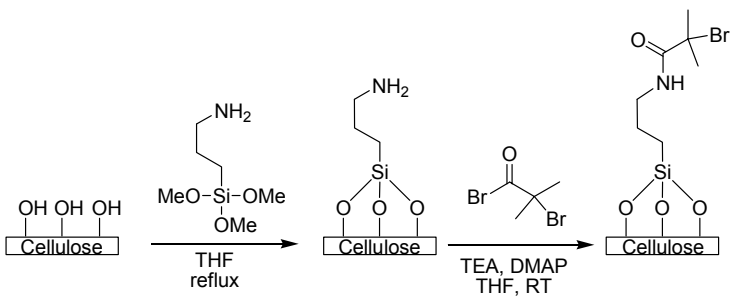

In order to incorporate a cleavable linker on the surface, the substrates were reacted with 3-aminopropyl-trimethoxysilane by refluxing for 48 h in a THF solution to yield silyl ether bonds (Scheme 4). The silane-functionalization was followed by immobilization of initiator as previously described.

3.3.2 Grafting from initiator-modified cellulose

The grafting reactions were generally conducted by immersing the initiator-modified cellulose substrate into a reaction mixture containing monomer, copper salt, ligand and solvent. In order to achieve control over the reactions, either sacrificial initiator or deactivator was added to the solution. The reaction mixture was then evacuated and back-filled with argon gas three times to remove oxygen.

3.3.2.1 Grafting of MA from intiator-modified cellulose

The grafting of MA from the initiator-modified substrates was performed at room temperature, catalyzed by Cu(I)Br/Me_6-TREN, similarly to the procedure developed by Carlmark and Malmström[64] (Scheme 5).

Scheme 5. Grafting of MA from initiator-modified cellulose.

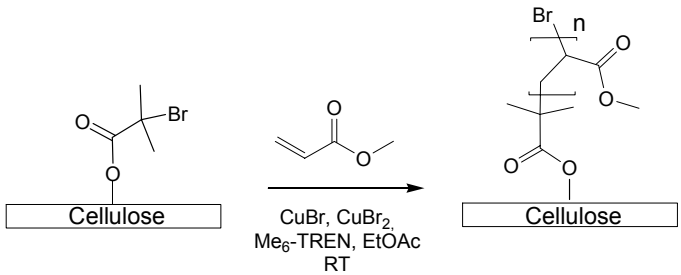

In order to achieve control over the reaction, the grafting was performed either with the addition of sacrificial initiator, ethyl 2-bromoisobutyrate, or by the addition of the deactivator, Cu(II)Br2. When sacrificial initiator was used, the grafts were targeted to different degrees of polymerization (DP) by adjusting the ratio of monomer to free initiator, and the reaction was allowed to proceed for 18 h. In the case when deactivator was added, the reaction was performed for 1-8 h. The PMA-grafted cellulose substrates were thereafter subjected to intense washing in THF, THF:water, water, dichloromethane, methanol and ethanol. The free polymer formed from the sacrificial initiator was dissolved in THF and passed through a column of aluminum oxide to remove the copper complex. The polymer was then dried under vacuum to remove solvent and remains of monomer.

3.3.2.2 Grafting of styrene from initiator-modified cellulose

The grafting of styrene from cellulose was performed in toluene, catalyzed by Cu(I)Br/N,N,N′,N′′,N′′-pentamethyldiethylenetriamine (PMDETA) at 90 °C according to Scheme 6. The polymerization was allowed to proceed for 18 h

Scheme 6. Grafting of styrene from initiator-modified cellulose.

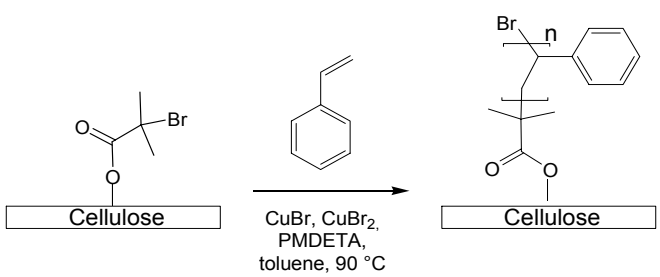

when the sacrificial initiator 1-phenyl ethyl bromide was added, and the DP was targeted to 100 and 300 respectively. Alternatively, the deactivator Cu(II)Br_2 was added to the reaction mixture, and the grafting reaction was performed for 1-8 h. The grafted-modified substrates were thereafter washed as previously described. The free polystyrene (PS) formed from the sacrificial initiator was dissolved in dichloromethane and passed through a column of aluminum oxide to remove the copper complex. The polymer was then precipitated in cold methanol and dried.

3.3.2.3 Grafting of MMA from initiator-modified cellulose

The grafting of MMA from initiator-modified cellulose was performed in toluene at 80 °C, catalyzed by Cu(I)Br/PMDETA as shown in Scheme 7.

When sacrificial initiator ethyl 2-bromoisobutyrate was added, the DP was targeted to 600 and the reaction was conducted for 1-18 h. When instead the deactivator, $CuBr_2$, was added to the reaction mixture, the polymerization was allowed to proceed for 2-4 h. The PMMA-grafted cellulose substrates were thereafter washed as previously described, and finally dried under vacuum. The free polymer formed from the sacrificial initiator was dissolved in dichloromethane and passed through a column of aluminum oxide to remove the copper complex. The polymer was then precipitated in cold methanol and dried.

Scheme 7. Grafting of MMA from initiator-modified cellulose.

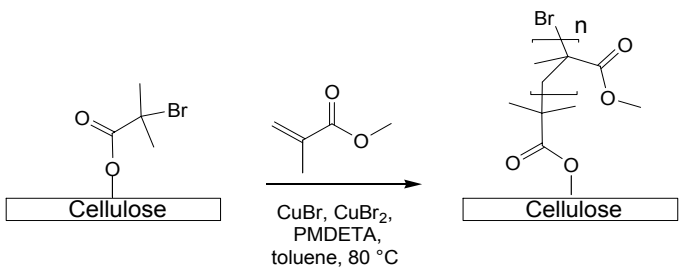

3.3.2.4 Grafting of GMA from initiator-modified cellulose

The grafting of GMA from the initiator-modified cellulose substrates was conducted in toluene at 30 °C, catalyzed by Cu(I)Cl/PMDETA (Scheme 8). $Cu(II)Br_2$ was added to achieve control over the reaction and the polymerization was allowed to proceed for 1-6 h. After the polymerization was completed, the PGMA-grafted cellulose substrate was thoroughly washed in THF, dichloromethane (DCM), methanol, THF/water and finally dried under vacuum.

Scheme 8. Grafting of GMA from initiator-modified cellulose.

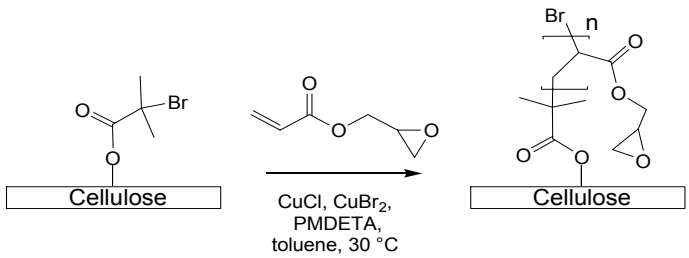

3.3.2.5 Grafting of NIPAAm from initiator-modified cellulose

The grafting of NIPAAm from initiator-modified cellulose substrate was conducted in $MeOH/H_2O$ at room temperature, catalyzed by Cu(I)Cl/ Me_6-TREN (Scheme 9). Deactivator, $Cu(II)Cl_2$, was added to achieve control over the reaction, and the polymerization was allowed to proceed for 15-60 min. The PNIPAAm-grafted substrates were thereafter washed as previously described, and finally dried under vacuum

Scheme 9. Grafting of NIPAAm from initiator-modified cellulose.

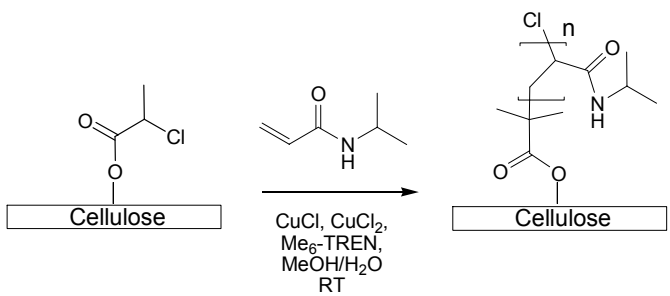

3.3.2.6 Grafting of 4VP from initiator-modified cellulose

The grafting of 4VP from initiator-modified cellulose substrates was conducted in 2-propanol at 50 °C, catalyzed by Cu(I)Cl/ Me_6-TREN according to Scheme 10. Deactivator, $Cu(II)Cl_2$, was added to achieve control over the reaction, and the polymerization was allowed to proceed for 2-6 h. The P4VP-grafted cellulose substrates were thereafter washed as previously described and finally dried under vacuum.

Scheme 10. Grafting of 4VP from initiator-modified cellulose.

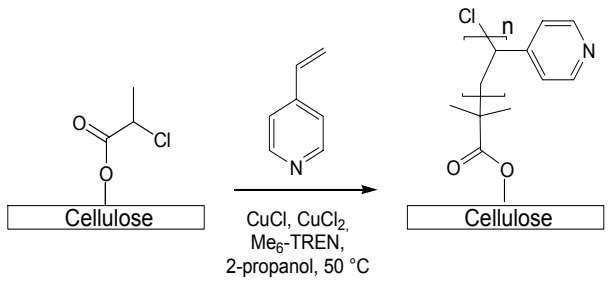

3.3.3 Cleavage of grafted polymer brushes.

Cleavage of grafted PMMA from a cellulose substrate was performed by treating the graft-modified substrates with tetrabutylammounium fluoride (TBAF) in a THF solution, in order to break the silyl ether linkages as shown in Scheme 11. The reaction was typically stirred for 5 h after which the cellulose

Scheme 11. Cleavage of grafted PMMA brushes.

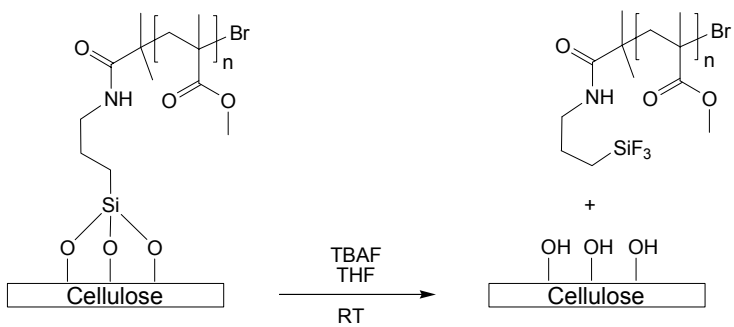

substrate was removed from the solution. The polymer-containing solution was concentrated and the polymer was precipitated in cold methanol over night. The precipitation was washed with methanol and centrifuged to isolate the polymer which was finally dried under vacuum.

3.3.4 Post-functionalization of grafted PGMA brushes

The epoxide groups in the PGMA-brushes are possible to react with a variety of compounds, and can thus be used for postfunctionalization of the graft-modified cellulose surfaces.

Scheme 12. Post-functionalization of PGMA-grafts with PDMS.

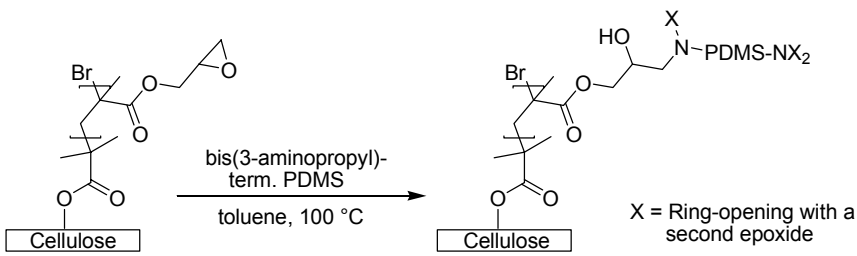

PDMS-functionalized PGMA-grafts were achieved by reacting the epoxide groups with bis(3-aminopropyl)-terminated PDMS in a solution of toluene according to Scheme 12. The reaction was allowed to proceed at 100 °C over night. The PDMS-functionalized cellulose surface was thereafter washed in toluene, THF, DCM and MeOH, and finally dried under vacuum.

In order to obtain hydroxyl groups available for further modification, the epoxide groups in the PGMA-grafted cellulose substrate were hydrolyzed using

Scheme 13. Hydrolysis of epoxide groups in PGMA-grafts.

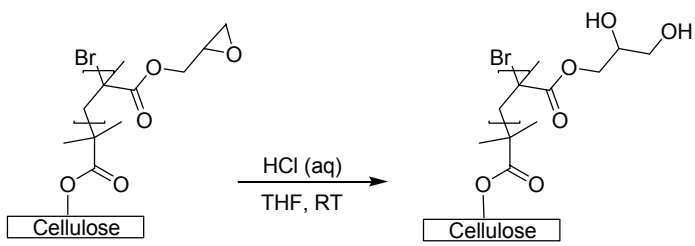

hydrochloric acid as shown in Scheme 13. The reaction was allowed to proceed for 45 minutes after which the cellulose substrate was washed in THF, methanol and ethanol and finally dried under vacuum. To enable a branched grafting architecture, the obtained hydroxyl groups were reacted as previously described, with 2-bromoisobutyryl bromide or 2-chloropropionyl chloride, to yield covalently bound ATRP initiators along the PGMA-brushes.

To obtain highly hydrophobic surfaces, the hydroxyl groups on the hydrolyzed PGMA-grafted cellulose substrate were reacted by immersing the substrate into a solution containing TEA and a catalytic amount of DMAP in DCM, followed by addition of pentadecafluorooctanoyl chloride, heptafluorobutyryl chloride or palmitoyl chloride (Scheme 14). The acylation was allowed to proceed at room temperature over night. The modified cellulose substrate was thereafter washed in DCM, THF and ethanol and finally dried under vacuum.

Scheme 14. Post-functionalization of hydrolyzed PGMA-grafts with acid chlorides.

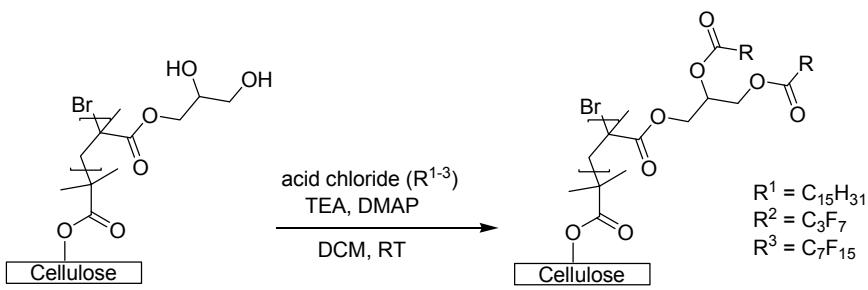

4 RESULTS AND DISCUSSION

4.1 SURFACE-INITIATED ATRP FROM BIO-FIBERS

The first aim of this study was to investigate the surface-initiated ATRP from a variety of different bio-fiber surfaces, and to study the influence of the substrate on the grafting. In order to fully characterize the grafted polymers, and to study the kinetics of the grafting reaction, it was necessary to develop a method for detaching the polymer brushes from the surface.

4.1.1 Preparation of graft-modified cellulose substrates

In order to enable the graft-modification of cellulose via ATRP, the hydroxyl groups on the surface of the substrate had to be converted into initiating sites. This was conducted by reaction of the hydroxyl groups with either 2-bromoisobuturyl bromide or 2-chloropropionyl chloride yielding covalently bound ATRP initiators on the surface, utilizing the procedure adopted from Carlmark and Malmström.[138] Attempts were made to analyze the initiator-modified substrates by FT-IR, but the low amount of ester group was undetectable with this method.

The grafting of various monomers from the initiator-modified substrates was conducted by immersion of the substrates into a reaction mixture containing monomer, ligand, copper halide and usually a solvent. To achieve control over the reaction, either sacrificial initiator or deactivator was added to the reaction mixture. Addition of a free sacrificial initiator allows for the possibility to pre-determine the graft lengths. The amount of initiating sites on the substrates is assumed to be negligible compared to the amount of free initiator, and the kinetics of the surface-initiated polymerization is assumed to be similar to that of the polymerization in the solution. Thus, the grafted polymers were targeted to different DP's by adjusting the monomer-to-free initiator ratio. Since the sacrificial initiator also initiates polymerization, a free polymer was formed simultaneously to the surface grafting. Analysis of the free polymer provides an indication of the molecular weight and polydispersity of the grafted polymer, assuming similar kinetics. However, it is necessary to separate the bulk polymer from the substrate resulting in a tedious work-up process. The grafted substrates were subjected to extensive washing and ultrasonication in various solvents to

assure complete removal of the bulk polymer. To ensure that the polymer was covalently attached to the substrates and not just physisorbed to the surface, blank samples were also prepared. In the blank samples the substrates were not reacted with initiator, but were otherwise treated in the same way as the initiator-modified samples. The blank samples were also used to determine when sufficient washing had been achieved.

FT-IR has proven to be a useful technique to characterize the grafted substrates. The spectra were normalized against a peak (typically around 1400 cm^{-1}) unaffected by the grafted polymer to make comparisons possible. Figure 7 displays the FT-IR spectra of MCC grafted with MA, targeting the DP to 100 and 300 respectively, compared to the blank sample and unmodified MCC. The grafting could be confirmed by the appearance of a carbonyl stretch peak at 1730 cm^{-1}. There is a significant increase in the peak intensity between DP 100 and 300, indicating that the graft lengths can be adjusted by varying the ratio of monomer to sacrificial initiator.

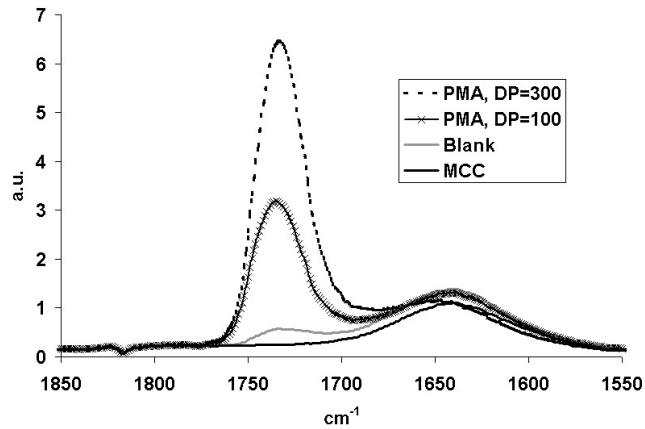

Figure 7. FT-IR spectra of PMA-grafted MCC to targeted DP 100 and 300.

When deactivator was added to achieve control over the reaction, the lengths of the grafts could only be controlled by the reaction time. The advantage with this method is that no free polymer is formed, and thus, the work-up procedure is straightforward.

4.1.2 Comparison between different substrates

Several types of polysaccharide substrates were chosen for this study to explore the feasibility of the grafting. Moreover, the purpose was to investigate how differences, in for instance surface area, between the substrates would influence the grafting. Native cellulose (filter paper and microcrystalline cellulose (MCC)), regenerated cellulose (dialysis membrane, and Lyocell fibers) and chitosan films were used as substrates.

Drying of polysaccharide substrates greatly affects the surface area and properties like swelling and solvent uptake. To reduce the differences between samples caused by drying, all the substrates were dried in a vacuum oven at 30°C over night prior to modification.

The substrates were grafted with MA using sacrificial initiator with targeted DP of 100. As can be seen in Figure 8, FT-IR analysis showed differences between the PMA-grafted substrates in the intensity of the carbonyl peak at 1730 cm^{-1}. The highest peak intensity is seen for MCC, which could be explained by the large surface area of this native cellulose substrate rendering dense grafts. The carbonyl peak is also high for filter paper, which also has a comparatively large surface area due to its fibrillar structure. The peaks are significantly lower for dialysis membrane and Lyocell fibers. These are both regenerated cellulose substrates, made by recrystallization of dissolved cellulose, which results in significantly lower surface areas than native cellulose substrates, affecting the

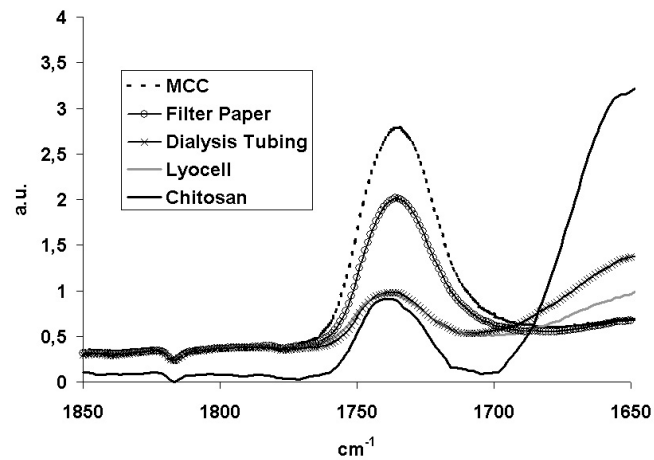

Figure 8. FT-IR spectra of PMA-grafted MCC, filter paper, dialysis tubing, lyocell and chitosan.

amount of grafted polymer on the surface. The hydroxyl groups are also less available for modification in these substrates, due to the irreversible drying, hornification, of the cellulose. As can be seen in Table 1, SEC analysis showed no significant difference in the molecular weight of the free polymers formed concurrently with the surface-initiated polymerizations from the different substrates, further indicating that the differences seen by FT-IR is due to grafting density and not graft lengths. The spectrum for the modified chitosan looks somewhat different from those of the cellulosic substrates, and therefore the baseline is different. In view of this, the carbonyl peak seems to be somewhere between the native and the regenerated cellulose substrates, even though the surface of the chitosan films is smooth. This indicates that the amino groups that structurally separate the chitosan from cellulose are more reactive than the hydroxyl groups. On the other hand, the bulk polymer formed when grafting from chitosan shows a higher molecular weight than the bulk polymers corresponding to the other substrates, which could explain at least some of the increased amount of grafted polymer in that sample.

Table 1. SEC results for free polymer formed during PMA-grafting of different substrates.

Substrate	M_n (g mol^{-1})	DP[a]	PDI
Filter Paper	6600	76	1.10
Dialysis membrane	6700	77	1.02
MCC	6700	77	1.15
Lyocell	6700	77	1.08
Chitosan	7800	90	1.03

[a]*The degree of polymerization was calculated from the SEC data.*

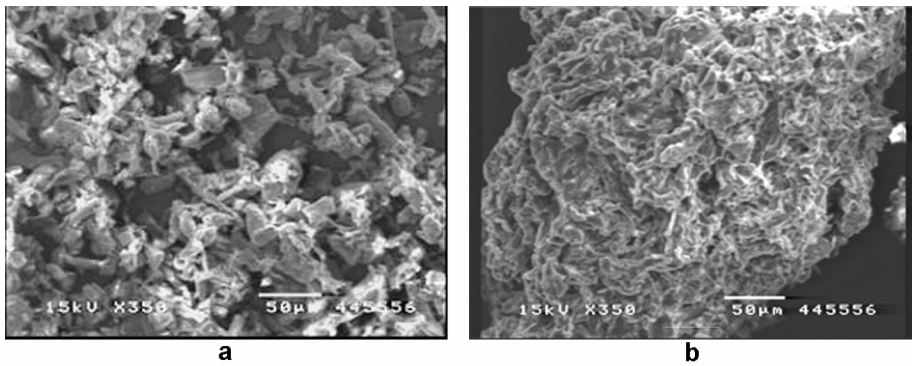

Figure 9. SEM images of a) unmodified and b) PMA-grafted MCC.

PMA-grafted MCC and Lyocell fibers were also characterized by SEM. Figure 9 shows the SEM-images of unmodified MCC and MCC grafted with MA for 8 h without sacrificial initiator, but with addition of deactivator. The modified MCC have aggregated into much larger particles than seen for the unmodified MCC. SEM-images of the corresponding unmodified and PMA-grafted Lyocell are shown in Figure 10. The surface of the unmodified fibers is very smooth compared with the modified fibers. The modified fiber surface seems to be partly covered with polymer and looks slightly more uneven.

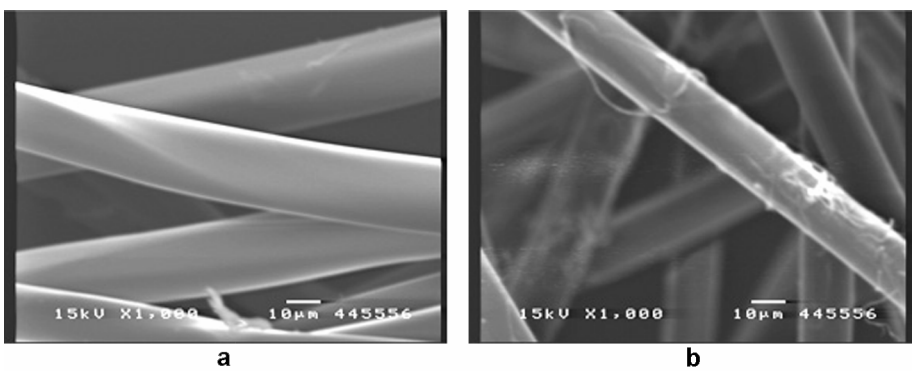

Figure 10. SEM images of a) unmodified and b) PMA-grafted Lyocell fibers.

4.1.3 Cleavage of grafted polymer

To study the surface-initiated polymerizations from cellulose, it is necessary to cleave the grafted polymer from the substrate. A few examples can be found in the literature on the cleavage of polymer brushes from a cellulose surface using acid- or base-catalyzed hydrolysis.[137,139,141] However, isolation of the detached polymer has shown to be difficult. The sensitivity of cellulose towards hydrolysis complicates the attempt to cleave polymers by the specific hydrolysis of ester bonds only at the initiating sites. The method of instead degenerating the cellulose by hydrolysis is a tedious process, and it is difficult to completely hydrolyze the cellulose chains and to isolate the polymer from the resulting solution. Furthermore, when attempting to cleave (meth)acrylates in this manner, there is a risk that also the grafted polymer is subjected to hydrolysis as it also contains ester linkages. To facilitate the cleavage, it was therefore decided to attach a functional group to the surface that could be cleaved selectively under conditions that left the cellulose and the polymer unaffected. A silyl group was attached to the filter paper, by reacting 3-aminopropyltrimethoxysilane with the hydroxyl groups on the cellulose surface according to Scheme 15, yielding silyl ether bonds which can be selectively cleaved using tetrabutylammonium fluoride (TBAF). The amine groups attached to the cellulose surface during the silane functionalization were thereafter reacted with 2-bromoisobutyrylbromide to yield covalently bound ATRP initiators on the surface (Scheme 15).

Scheme 15. Synthetic approach to attachment of cleavable linkage, grafting of PMMA and cleavage of grafted polymer chains.

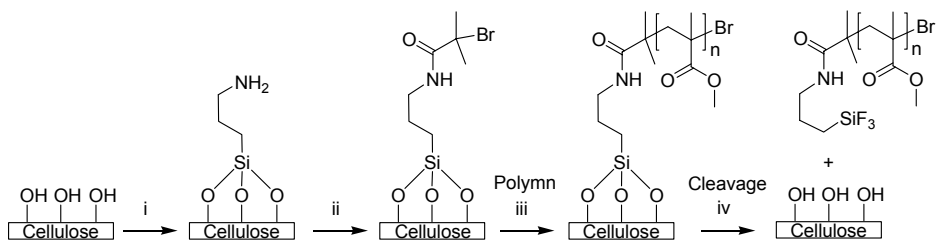

[a]Conditions: i) 3-aminopropyltrimethoxysilane, THF, reflux; ii) 2-bromoisobutyryl bromide, TEA, DMAP, THF, room temperature; iii) MMA, CuBr, $CuBr_2$, PMDETA, toluene, 80 °C; iv) TBAF, THF, room temperature.

Graft-modification of the cellulose substrates with MMA was performed at 80 °C, targeting the DP to 600 for all grafting reactions, by adjusting the ratio of monomer to sacrificial free initiator. However, to study the kinetics of the polymerization the reaction time was varied between 1-18 h to allow the

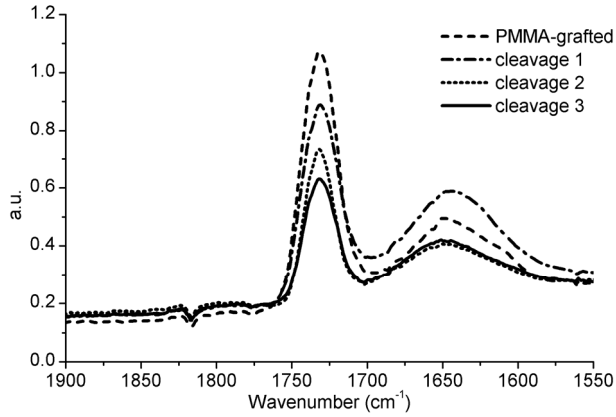

Figure 11. FT-IR spectra of PMMA-grafted cellulose before and after the first, second and third cleavage reaction.

polymerization to proceed to different monomer conversions as determined by ^{1}H NMR. Graft-modification of the cellulose with MMA was also performed without sacrificial initiator. The deactivator Cu(II)Br$_2$ was then added to the reaction mixture to control the reaction, and the length of the grafts was controlled by varying the reaction time.

The grafted PMMA was cleaved from the substrate using TBAF to break the silyl ether bond, as shown in Scheme 15. To obtain a sufficient amount of cleaved polymer for SEC analysis, the reaction was repeated and could be followed and confirmed by FT-IR analysis by the decrease in the carbonyl peak at 1730 cm^{-1} for each cleavage reaction, as can be seen in Figure 11. After stopping the reaction,

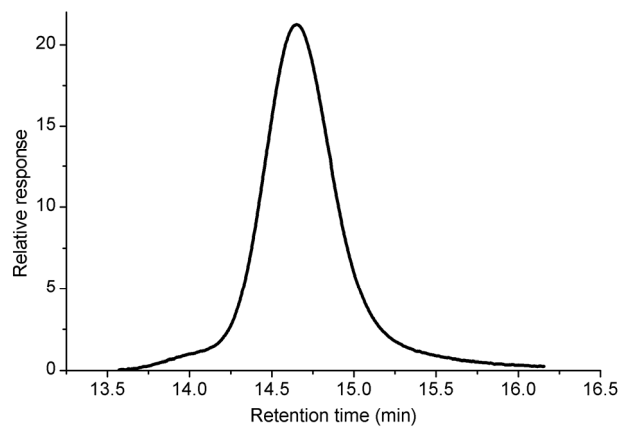

Figure 12. SEC trace of cleaved PMMA; targeted DP = 600, 44% monomer conversion, M_n = 25 500 g mol^{-1}, PDI = 1.08.

the filter paper was removed from the flask and the cleaved polymer was precipitated in MeOH to remove the excess of TBAF, and analyzed by SEC and ^{1}H NMR. SEC analysis of cleaved PMMA grafted from filter paper to a monomer conversion of 44% showed M_n = 25 500 g mol^{-1} and PDI = 1.09 indicating a controlled polymerization, Figure 12. The molecular weight of the cleaved polymer was very similar to that of the corresponding free polymer of 25 100 g mol^{-1} with PDI = 1.16.

The cleavage reaction is stoichiometric, and it is important not to use a too large excess of TBAF as the cellulose then was found to be deteriorated. This has previously been reported for the treatment of cellulose with hydrogen fluoride.[142] Using a moderate excess of TBAF in THF, however, seems to cleave the polymer without affecting the cellulose. Analyzing the cleaved PMMA with ^{1}H NMR showed that the methyl esters in the polymer had not been affected by the TBAF treatment, Figure 13. This makes the technique advantageous to the hydrolysis methods by which it is difficult to cleave only the ester bond between the surface and the grafts without cleaving hydrolysis-sensitive bonds present in the grafted polymer. A sample of free PMMA was also analyzed with SEC before and after treatment with TBAF, showing no effect on molecular weight and PDI. To ensure that no fractionation of the cleaved polymers had occurred due to the precipitation, cleaved polymer samples were also analyzed by SEC without previous precipitation, showing controlled polymerizations also for these samples.

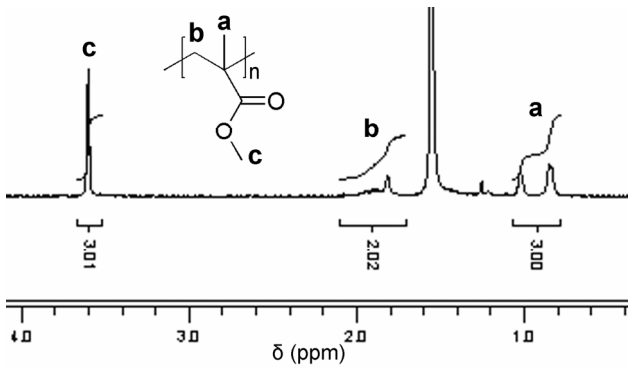

Figure 13. ^{1}H NMR spectrum of cleaved PMMA.

FT-IR analysis of the cellulose surface showed a significant decrease in carbonyl peak intensity after the cleavage reactions; however, it was not possible to cleave off the total amount of grafted polymer from the surface. This could be due to the fact that the silane reagent might be less reactive towards the hydroxyl groups on the surface than the acyl bromide attached to create ATRP initiators.

The acyl bromide could react not only with the amine groups on the silane-functionalized surface, but also with hydroxyl groups that are unavailable for the silane. This would leave ATRP initiators attached also directly to the surface, and not only to the silanes. Polymer grafted from these initiating sites would not be possible to cleave off using TBAF, which would explain the observed uncleaved part of the grafted polymer sample.

4.1.4 Kinetics of the grafting reaction

To study the kinetics of the surface-initiated polymerization, the PMMA grafted from the cellulose surfaces to different monomer conversions was cleaved for all samples, and the molecular weights of grafted and free PMMA could be compared (Figure 14, Table 2). As can be seen, the PDI values are below 1.4 for all the samples, indicating controlled polymerizations.

Table 2. Molecular weight and PDI for cleaved and free polymer at different monomer conversions.

Conv.[a] (%)	$M_{n,cleaved}$ **(g mol^{-1})**	$M_{n,free}$ **(g mol^{-1})**	**PDI$_{cleaved}$**	**PDI$_{free}$**
29	26 200	17 300	1.13	1.12
30	24 600	13 000	1.14	1.12
44	25 500	25 100	1.11	1.09
58	34 400	32 800	1.08	1.14
75	42 800	40 100	1.20	1.10
87	46 300	42 300	1.27	1.13

[a]*Monomer conversion calculated from ^{1}H NMR*

The molecular weights of the grafted polymers are similar to the free polymers at higher monomer conversions. However, at monomer conversions below 40% the molecular weights of the cleaved polymers are higher than the free polymers, indicating that the reaction in the beginning proceeds faster from the surface than in the solution and then slows down. In the beginning of the grafting reaction the copper complex appears to be drawn to the filter paper surface and a green precipitation can be observed on the surface. This suggests that the concentration of the catalyst then is higher at the surface, causing the reaction to proceed faster there than in the solution. After some time, the polymer grafts are long enough to cover the cellulose surface and the environment for the propagating chain ends then become more similar to those of the growing polymer chains in the solution, which causes the kinetics of the

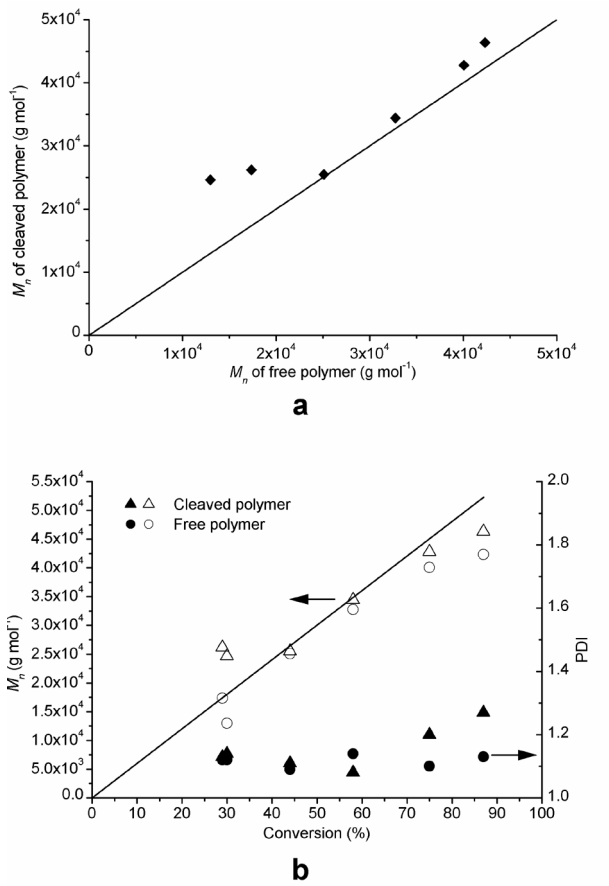

Figure 14. Relationship of molecular weight between cleaved PMMA and free PMMA formed by sacrificial initiator (a), and dependence of molecular weight and PDI on monomer conversion for cleaved and free PMMA (b). Solid lines are theoretical values.

solution polymerization and the surface-initiated polymerization to become comparable. The molecular weight of the grafted and free polymer is still similar but no longer increasing linearly at monomer conversions of 75% and above. SEC analysis of cleaved polymer grafted to monomer conversion of 75% and above showed increasingly bimodal traces. The molecular weight corresponding to the second peak is about twice of the molecular weight for the main part of the sample indicating that parts of the polymer grafts have been terminated by inter-chain coupling during the polymerization. At high monomer conversions the reaction mixture becomes increasingly viscous, increasing the probability of termination *via* recombination. Furthermore, it could be observed that the

viscosity was higher in the close proximity to the substrates than in the solution, as the free polymer was sedimented there. The polymerization from the surface therefore becomes diffusion controlled at lower monomer conversions than the polymerization in the solution. This, in combination with the already short distance between the chain ends of grafted polymers could explain the increased amount of termination of the surface-initiated polymerization compared to the solution polymerization.

SEC analysis of cleaved polymer from separate cleavage reactions on the same sample showed increasingly bimodal traces, indicating that it is more difficult to cleave off the terminated chains. This could be due to the fact that the recombined chains are attached in two ends, generating more bonds that need to be cleaved to effectively detach the polymer chain. This implies that the termination occurs via inter-chain coupling between grafts on the surface rather than between grafted and free polymer.

4.2 FUNCTIONAL CELLULOSE SURFACES

4.2.1 Superhydrophobic cellulose

Superhydrophobic surfaces can be obtained by modification of a rough material with low energy compounds, such as fluorine. The first attempt to create a superhydrophobic cellulose surface was therefore to attach a fluoroalkyl

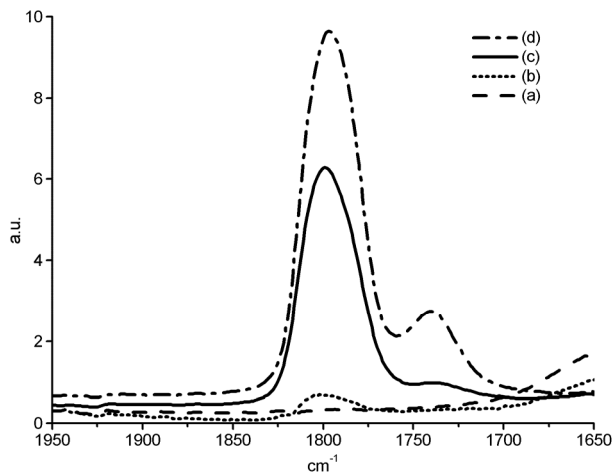

Figure 15. FT-IR spectra of a) unmodified cellulose, b) fluorinated cellulose, c) fluorinated PGMA-grafted cellulose, and d) fluorinated "graft-on-graft"-modified cellulose.

chain to a filter paper with high inherent roughness. This was accomplished by reacting the hydroxyl groups on the surface with pentadecafluorooctanoyl chloride. FT-IR analysis could confirm the acylation reaction by the appearance of a carbonyl peak at 1800 cm^{-1}, not seen for unmodified cellulose (Figure 15a-b).

Static water contact angle measurements revealed a hydrophobic surface after modification. However, the exact contact angle (CA) is somewhat difficult to determine due to the inherent roughness of the cellulose surface. The modified surface first seemed to be superhydrophobic, as the obtained CA was around 150°. However, it was observed that the water droplet was gradually adsorbed into the surface over time, suggesting an insufficient surface-coverage.

Scheme 16. Synthetic approach for functionalization of cellulose substrate.[a]

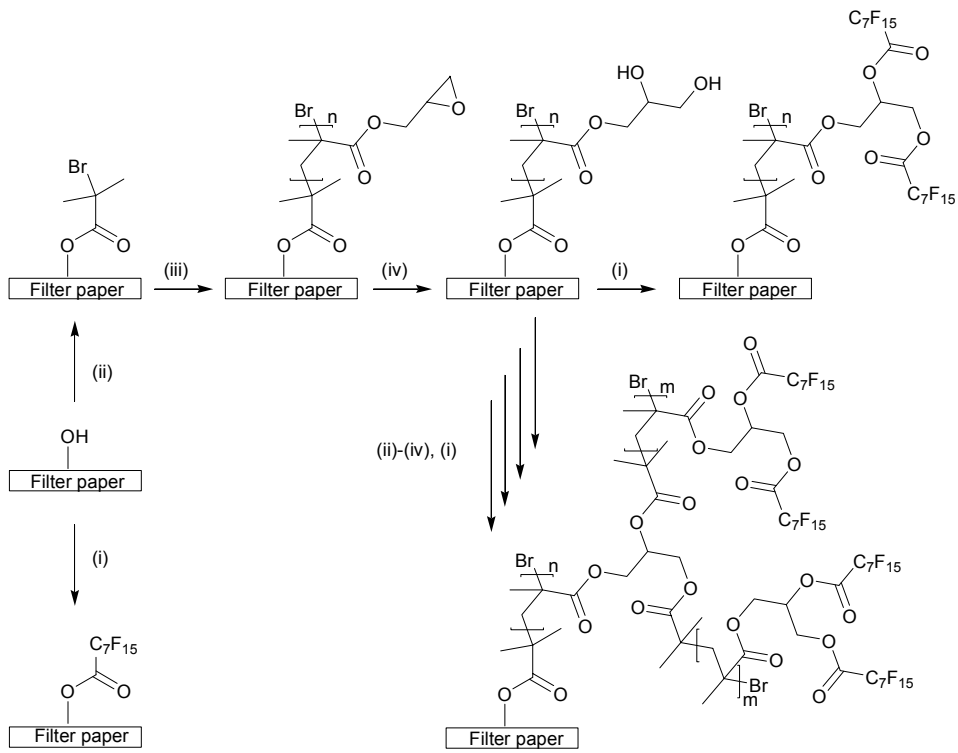

[a]*Conditions: i) pentadecafluorooctanoyl chloride, TEA, DMAP, DCM, RT; ii) 2-bromoisobutyryl bromide, TEA, DMAP, THF, RT; iii) GMA, CuCl, $CuBr_2$, PMDETA, toluene, 30 °C; iv) HCl(aq), THF, RT.*

In order to improve the surface-coverage and thereby the hydrophobicity, the functional monomer glycidyl methacrylate (GMA) was grafted from the cellulose substrate to enable attachment of an increased amount of fluorine groups. The grafting of GMA from the cellulose substrate was conducted in toluene at 30 °C, catalyzed by Cu(I)Cl/Cu(II)Br_2/PMDETA, and could be confirmed from FT-IR analysis by the appearance of a carbonyl stretch at 1730 cm^{-1} (Figure 15c) The pendant epoxide groups in the PGMA-grafts were hydrolyzed under acidic conditions to obtain hydroxyl functional polymer brushes. The hydrolysis was confirmed by the increased wettability of the surface, and also *via* FT-IR analysis, where a shift in the carbonyl stretch could be observed. Fluorination of the hydroxyl functional grafts was accomplished by reaction with pentadecafluorooctanoyl chloride. FT-IR analysis showed a second carbonyl stretch at 1800 cm^{-1}, confirming the attachment of fluorine groups, as can be seen in Figure 15c. A CA of 161° was observed for the fluorinated PGMA-grafted filter paper, which is an improvement compared to the direct fluorination route. Furthermore, the stability over time for the CA was improved, suggesting that an increased surface coverage was obtained from the graft-modification. The CA decreased from 161° to 138° during 1 h, meaning that the surface was still highly hydrophobic, however not superhydrophobic, after that time. The improvement in CA by the graft-modification is, however, small compared to the increase in the number of fluorine groups attached to the

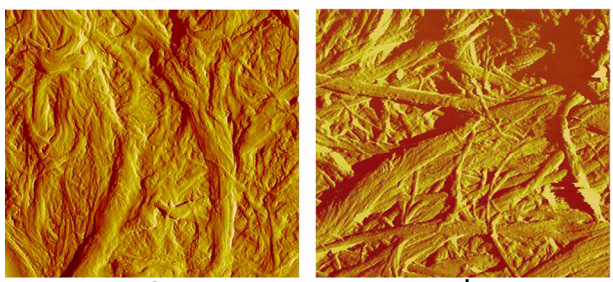

Figure 16. AFM amplitude images (5 x 5 µm) of a) fluorinated cellulose substrate, and b) fluorinated PGMA-grafted cellulose substrate.

surface, as can be seen in the FT-IR spectra in Figure 15a-c. This could be explained by the fact that the hydrophobicity of a surface is dependent not only on its chemical composition, but also on the topography. The surface roughness of the substrates prepared by the two modification routes was analyzed with tapping-mode AFM (Figure 16). The fibrillar structure resembling that of an unmodified surface can still be seen for both substrates. For the sample where

the fluorine groups were attached directly, the surface appears more compact. When GMA was grafted from the substrate and subsequently ring-opened and fluorinated, the surface appears less dense. This might indicate that the grafting process affects the interfibrillar interactions, giving rise to exposure of non-modified regions, which could explain the relatively low increase in CA for this surface.

In order to further increase the CA and to obtain a stable superhydrophobic surface, a new route that generated higher surface roughness and enabled the attachment of larger amounts of hydrophobic compounds was explored. Immobilization of 2-bromoisobutyryl bromide was conducted on the hydrolyzed, hydroxyl functional PGMA-brushes, to generate polymer grafts containing a multitude of initiators along the back-bone of each chain. A "graft-on-graft" architecture was obtained when GMA was polymerized from the initiating sites on each graft (Scheme 16). Post-functionalization of the "graft-on-graft"-modified cellulose surface was carried out thereafter, and FT-IR confirmed the attachment of a very high number of fluorine groups (Figure 15). The resulting surface showed extremely high CA, reaching a maximum of 172°. The hysteresis was below 5°, thus indicating a Cassie-Baxter hydrophobic state in which a non-sticky surface is expected. (Table 3). The CA remained almost constant over time and the surface was still superhydrophobic after 1 h.

According to AFM analysis, the fluorinated "graft-on-graft"-modified substrates show a rough surface structure, as can be seen in Figure 17. The surface is clearly covered by the polymer; however, the fibrils are still visible providing a micro structure. Overlaying the fibrillar structure, nano-sized features are distinguished, demonstrating that the surface exhibits a micro-nano-binary structure. This kind of surface structure, in combination with a hydrophobic waxy material, has been proposed to explain the superhydrophobic and self-cleaning effects of the Lotus leaf.

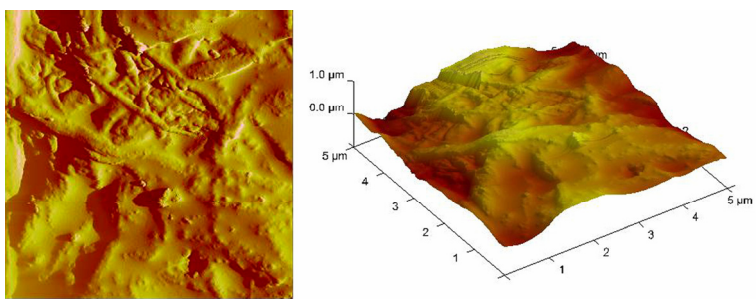

Figure 17. AFM amplitude image, 5 x 5 µm (left), and mixed surface plot (right) of fluorinated "graft-on-graft"-modified cellulose surface.

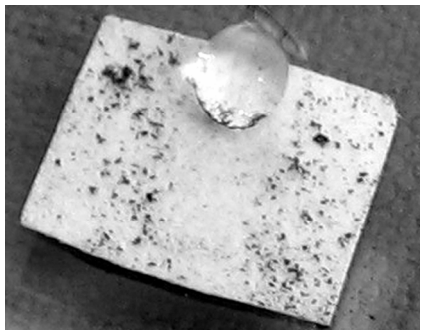

Figure 18. Demonstration of self-cleaning ability of the fluorinated "graft-on-graft"-modified cellulose substrate.

The self-cleaning ability of the modified cellulose substrates was also investigated. After contamination of the surface with carbon black powder, the water droplets applied to the surface collected the powder. The "dirt-containing" water droplets rolled off the surface as soon as the filter paper was tilted, leaving a clean surface, as can be seen in Figure 18. To further verify the superhydrophobic nature of the surface, a water droplet was allowed to fall onto the surface. The droplet was observed to bounce back up after impact with the surface, meaning that the surface acts as a spring for the droplet (Figure 19).

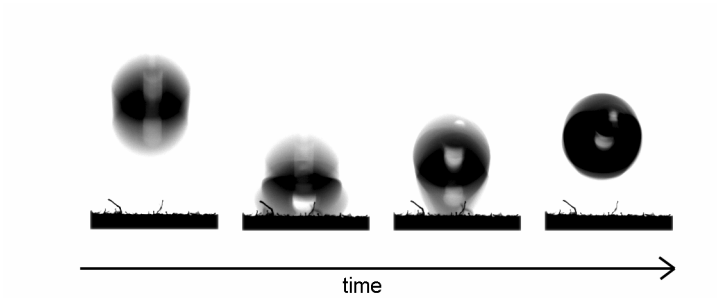

Figure 19. Water droplet bouncing back up from fluorinated "graft-on-graft"-modified cellulose surface after impact (approximately 10 ms between each image).

4.2.1.1 Post-functionalization to yield reduced fluorine amounts

Since fluorine-containing compounds are expensive, and also known to affect the nature negatively, the possibility to obtain highly hydrophobic materials using reduced amounts, or even complete removal of fluorine groups was investigated.

Reduction of the fluorine amount was achieved by attachment of a shorter fluoroalkyl chain to the "graft-on-graft"-modified substrates by post-functionalization using heptafluorobutyryl chloride. The resulting surface showed similar characteristics as the surface post-functionalized with the longer fluoroalkyl chains (Table 3).

Table 3. Results from contact angle measurements for different post-functionalizations on "graft-on-graft"-modified cellulose surfaces.

Surface functionalization	Contact Angle			
	Static	Adv.	Rec.	Hysteresis
PGMA-*g*-PGMA-PDMS	162°	164°	154°	10°
PGMA-*g*-PGMA-$C_{15}H_{31}$	165°	167°	162°	5°
PGMA-*g*-PGMA-C_3F_7	162°	164°	156°	9°
PGMA-*g*-PGMA-C_7F_{15}	172°	173°	168°	5°

To fabricate a superhydrophobic bio-fiber surface completely without fluorinated compounds, the use of biocompatible and hydrophobic polydimethylsiloxane (PDMS) was investigated. Bis(3-aminopropyl) terminated PDMS was reacted directly with the epoxide groups in the branched PGMA-grafts, and the reaction could be confirmed by FT-IR from the appearance of a peak at 805 cm^{-1} corresponding to the siloxane groups. The PDMS-modified surface had a CA of 162°, showing that superhydrophobic surfaces could also be obtained without the use of fluorine (Table 3). AFM analysis revealed that the PDMS-functionalized surfaces showed a smoother surface topography as compared to the surface functionalized with the fluoroalkyl chain. Furthermore, no nano-sized features could be observed for this surface. The smoother surface structure could be explained by the high molecular weight of PDMS compared to the fluorinated acyl chloride. In addition, each amine in the PDMS end groups may react with two epoxide groups, forming a cross-linked network which will contribute to the smooth surface structure.

Post-functionalization with long alkyl chains ($C_{15}H_{31}$) was also conducted by reaction of the hydroxyl functional branched PGMA-brushes with palmitoyl chloride. FT-IR analysis of the alkyl-functionalized surfaces showed an increase in intensity of the carbonyl peak at 1730 cm^{-1} The CA was measured to 165° and

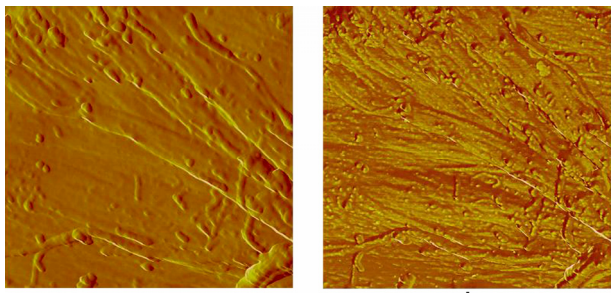

Figure 20. AFM images of alkyl-functionalized "graft-on-graft"-modified cellulose surface (5x5 μm); a) amplitude, and b) phase image.

showed stability over time, and low hysteresis (Table 3). AFM-analysis of the alkyl-functionalized cellulose substrate showed a similar surface structure to the fluoroalkyl-functionalized surface. The fibrils are almost completely coverered and both micro- and nano-sized features can be observed (Figure 20) The nano-sized features were even more pronounced in the AFM phase image of this sample compared to the fluoroalkyl-functionalized surface, which might be explained by the difference in modulus between the polymers in the "graft-on-graft" structure and the attached alkyl chains (Figure 20b).

4.2.2 Stimuli-responsive cellulose surfaces

Stimuli-responsive cellulose surfaces were obtained by graft-modification of filter paper with *N*-isopropylacrylamide (NIPAAm) and 4-vinylpyridine (4VP) to yield thermo- and pH-responsive polymer brushes, respectively. Block-copolymer brushes of PNIPAAm and P4VP grafted from bio-fiber substrates rendered dual-responsive surfaces.

4.2.2.1 Thermo-responsive bio-fiber surfaces

The surface-initiated ATRP of NIPAAm to produce thermo-responsive polymer brushes was performed in a solution of MeOH/H_2O and catalyzed by Cu(I)Cl/Cu(II)Cl_2/Me_6-TREN. The grafting reactions were conducted at ambient temperature for 15-60 min. Swelling of the substrate was observed for longer

reaction times. This can be explained by the formation of hydrogen bonds between PNIPAAm and cellulose, breaking up the interfibrillar structure that is also held together by hydrogen bonding, causing the cellulose fibrils to separate

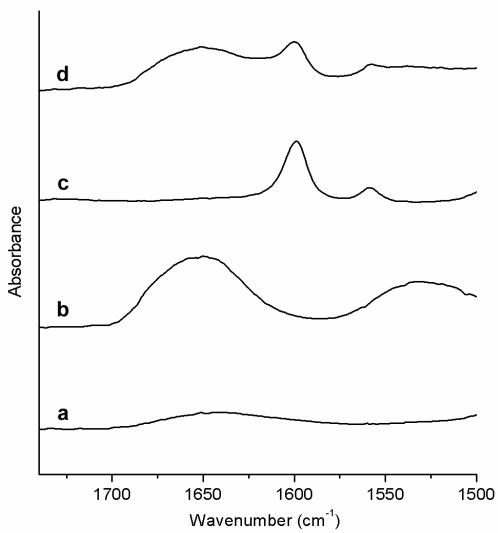

Figure 21. FT-IR spectra of cellulose substrate; a) unmodified, b) PNIPAAm-grafted, c) P4VP-grafted, and d) P4VP-b-PNIPAAm-grafted.

from each other. FT-IR analysis of the PNIPAAm-grafted cellulose surfaces showed the amide I-II peaks at 1650 cm^{-1} and 1540 cm^{-1} confirming the reaction, Figure 21b.

The PNIPAAm-grafted cellulose surface exhibited wettability variations in response to changes in temperature due to the LCST of the polymer at 32 °C according to Figure 22. Below LCST, the PNIPAAm brushes assume a stretched conformation due to inter-molecular hydrogen-bonding with water, resulting in a hydrophilic behavior. However, above LCST the brushes undergo a phase-transition resulting in a collapsed conformation due to intra-molecular hydrogen bonding, resulting in reduced wettability of the surface.

The wettability of the PNIPAAm-grafted cellulose surfaces was characterized by static contact angle (CA) measurements at different temperatures. The modified bio-fiber surface was hydrophilic below LCST and, as expected, the applied water droplet was adsorbed into the surface. At temperatures above LCST, a water droplet applied to the surface had a CA of 110°; however, it was gradually adsorbed into the surface. The stability of the CA decreased with

increasing graft length, indicating that the effect of the NIPAAm grafting on the interfibrillar structure is causing unmodified areas to be exposed.

In order to avoid the exposure of hydrophilic unmodified areas and to obtain higher grafting density, PNIPAAm was grafted from iniator-functionalized PGMA brushes, resulting in a branched "graft-on-graft" architecture on the bio-fiber surface. The resulting surface was hydrophilic under LCST; however, above LCST, the modified bio-fiber surface was hydrophobic with a stable CA of 130°, thus indicating a less affected interfibrillar structure from the NIPAAm grafting due to a protecting PGMA layer. Furthermore, this suggests that the PGMA layer is not affecting the thermo-responsivity of the surface.

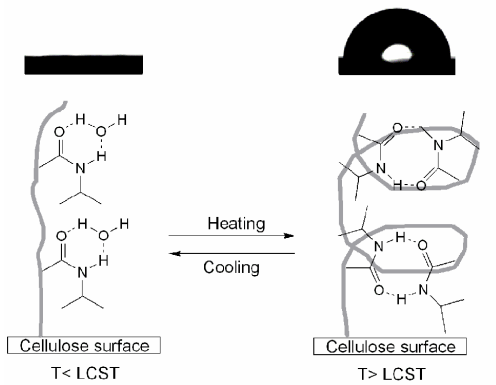

Figure 22. Wettability changes of the PNIPAAm-grafted cellulose surface due to conformation changes of the brushes below and above LCST.

4.2.2.2 pH-responsive bio-fiber surfaces

The grafting of 4VP from the initiator modified cellulose surface to produce pH-responsive brushes was performed in 2-propanol catalyzed by Cu(I)Cl/Cu(II)Cl_2/Me_6-TREN as this system has been shown to reduce coordination of the copper halide to the pyridyl groups and minimize unwanted side-reactions.[143,144] The grafting reactions were performed at 50 °C for 2-6 h. FT-IR analysis confirmed the success of the grafting of P4VP from cellulose by the appearance of peaks at 1597 and 1556 cm^{-1}, corresponding to the pyridyl ring-stretching, Figure 21c.

The P4VP-grafted cellulose surfaces responded to changes in pH due to the protonation and deprotonation of the pyridyl group, Figure 23. In the protonated state, the brushes exhibit an extended coil conformation due to electrostatic

repulsion of the charged pyridinium segments. However, a collapse of the brushes occurs with de-protonation at pH ≥5 (pKa~5.2). This transition is reflected by changes in the wettability of the surface. The P4VP-modified cellulose surfaces were characterized by static CA measurements at pH 3, 7 and 9, respectively. At pH 3, the P4VP-modified cellulose surface is hydrophilic, and the applied water droplet is adsorbed into the surface within a couple of seconds. Protonation of the pyridine ring was confirmed by FT-IR measurements and resulted in a shift of the peaks corresponding to the pyridyl group to 1638 and 1605 cm^{-1}, respectively, as earlier reported by Ruokolainen *et al.* and Li and co-workers.[145,146] The hydrophobic character is greatly enhanced in the deprotonated state at pH 9 resulting in CA of 125°. However, the cellulose surface with longer

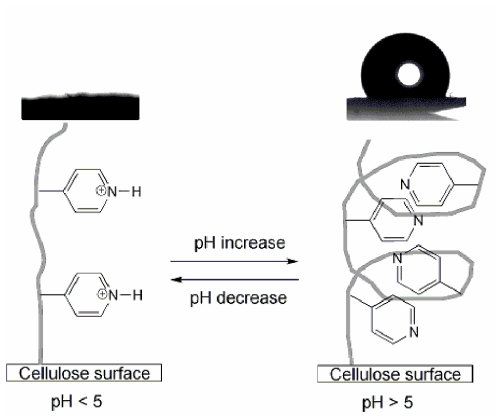

Figure 23. Wettability changes of the P4VP-grafted cellulose surface due to protonation and deprotonation of the pyridyl group.

P4VP brushes showed a decreased CA of about 103°. This could be explained by the fact that longer polymer grafts result in a smoother surface, which would decrease the CA as the surface roughness is an important parameter for hydrophobicity.

At pH 7, the P4VP-grafted substrates overall exhibit lower CA's (90-100°) than at pH 9. The CA's were, however, not stable at this pH, and different values were obtained at different measurements for the same sample. This suggests that the deprotonation of the pyridyl group is incomplete at this pH, resulting in regions of more hydrophilic and hydrophobic character, respectively.

4.2.2.3 Dual-responsive bio-fiber surfaces

In order to create surfaces that respond to two different separate triggers (pH and temperature), PNIPAAM-*b*-P4VP and P4VP-*b*-PNIPAAM block-copolymer brushes were grafted from the cellulose substrates. The appearance of the amide peaks at 1650 cm^{-1} and 1540 cm^{-1}, and the pyridyl peaks at 1597 cm^{-1} and 1556 cm^{-1} from FT-IR analysis confirmed the formation of block copolymer brushes, Figure 21d. The successful polymerization of a second block, using the graft-modified cellulose surfaces as macro-initiators, furthermore proofs the presence of living chain ends in the first block, and thus a controlled polymerization of NIPAAm and 4VP, respectively.

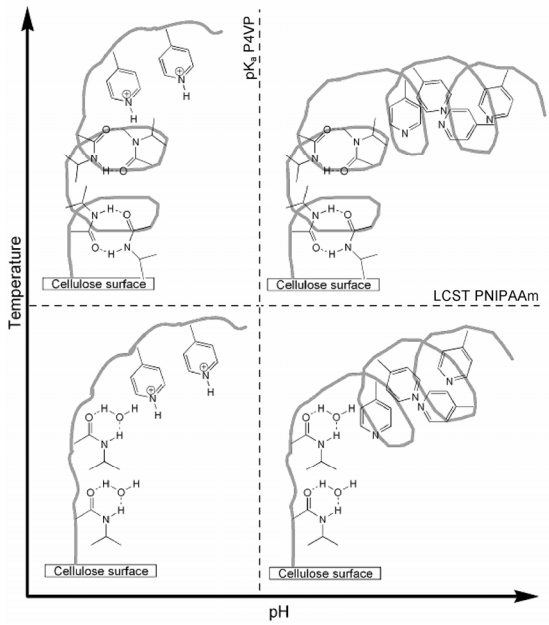

Figure 24. Conformation of dual-responsive block-copolymer brushes at different pH and temperature.

Table 4 displays the results from the CA measurements on the block copolymer modified cellulose surface at pH 3 and 9, at temperature below and above the LCST of PNIPAAm. At room temperature, the PNIPAAm block exhibits an extended conformation due to intermolecular hydrogen bonding with water, and the P4VP block changes conformation with variations in pH, as illustrated in Figure 24. At pH 3 and room temperature, the pyridine segments in the P4VP block are protonated, and both of the blocks exhibits extended conformation. Under these conditions, all the surfaces are hydrophilic, and the

applied droplet is rapidly adsorbed into the substrate. At pH 9 and room temperature, the P4VP block becomes deprotonated resulting in a collapsed conformation, whereas the PNIPAAm block is extended. As can be seen in Table 4, the surfaces grafted with PNIPAAm-*b*-P4VP are hydrophilic when the PNIPAAm block is long and the P4VP block is short. This could be due to incomplete surface coverage of the relatively short P4VP block in combination with disrupted interfibrillar structure caused by the PNIPAAm grafting. Alternatively, the hydrophilic character of the surface may be caused by rearrangement of the brushes to expose the hydrophilic PNIPAAm block. When the PNIPAAm block is short and the P4VP block long, the surface is hydrophobic, indicating a more complete coverage of the surface with the P4VP block. In the case when P4VP is grafted as the first block from the cellulose substrate (P4VP-*b*-PNIPAAm), the CA is about 100° independently of block lengths. It is suggested that the grafting of P4VP results in a less affected fibrillar structure of the bio-fiber surface compared to PNIPAAm, which swells the substrate exposing unmodified regions. This increased surface coverage could explain the increased hydrophobicity of P4VP-*b*-PNIPAAm compared to the reverse order of the blocks.

Table 4. Contact angles at different pH for graft-modified cellulose at room temperature (below LCST) and at elevated temperature (above LCST).

Brush type	t_{R1}[a] **(min)**	t_{R2}[b] **(min)**	**CA**			
			pH 3	**pH 3 T>LCST**	**pH 9**	**pH 9 T>LCST**
PNIPAAm-*b*-P4VP	15	360	0	0	100°	115°
PNIPAAm-*b*-P4VP	30	120	0	85°	0	120°
PNIPAAm-*b*-P4VP	60	120	0	65°	0	115°
P4VP-*b*-PNIPAAm	120	30	0	0	100°	115°
P4VP-*b*-PNIPAAm	360	15	0	0	100°	115°

[a]*Reaction time for the polymerization of the first block.* [b]*Reaction time for the polymerization of the second block.*

When the temperature is increased to above the LCST of PNIPAAm, the PNIPAAm block exhibits a collapsed conformation due to intramolecular hydrogen bonding, and the P4VP block changes conformation with changes in pH, as can be seen in Figure 24. At pH 3, and above LCST, the P4VP block is extended and the PNIPAAm block is collapsed. The substrate grafted with PNIPAAm-*b*-P4VP with a short PNIPAAm block and a long P4VP block is hydrophilic under these conditions, indicating that the hydrophilic character of P4VP is dominant in this case. The longer PNIPAAm blocks, combined with a

short P4VP block, result in a reduced wettability of the surface; however, the resulting CA's are lower than 90°, indicating that the surfaces are hydrophilic. This suggests competing influence from both blocks over the surface wettability. When instead P4VP was grafted as the first block from the substrate (P4VP-*b*-PNIPAAm), the surfaces are hydrophilic at high temperatures at pH 3, indicating that the P4VP block is longer than the PNIPAAm block in these cases, resulting in a dominant hydrophilic effect. This could also be explained by a rearrangement of the brushes to expose the hydrophilic P4VP block. At pH 9, and above LCST, both blocks are supposed to be in the collapsed conformation and as expected, all the surfaces were hydrophobic. However, the PNIPAAm-*b*-P4VP modified samples showed less stable CA's than for the surfaces with P4VP as the first block. This is probably also an effect of the affected interfibrillar structure caused by the PNIPAAm grafting.

The reversibility of the wettability for the P4VP-b-PNIPAAm modified surfaces was demonstrated by cycling between pH 3 at room temperature and pH 9 at elevated temperature several times, showing similar CA, Figure 25.

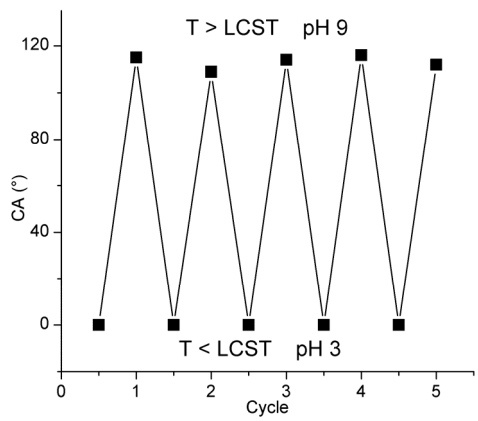

Figure 25. Contact angles at different temperature and pH for a P4VP-b-PNIPAAm-modified cellulose surface. Half cycles: T < LCST, pH 3; and integral cycles: T > LCST, pH 9.

5 CONCLUSIONS

Surface-initiated ATRP has been explored as a tool for surface modification of various bio-based substrates. A variety of hydrophobic and hydrophilic monomers have been grafted from the substrates. It has been shown that the surface area and morphology significantly affects the amount of grafted polymer. Native cellulose substrates have a higher surface area, making it possible to graft denser brushes than from a smooth regenerated cellulose surface.

The kinetics of the surface-initiated polymerization of methyl methacrylate from cellulose have been studied by the successful cleavage of PMMA from the surface. Detachment of the polymer was enabled by the incorporation of a selectively cleavable silyl ether bond. SEC analysis showed PDI values as low as 1.08 for the detached polymer, indicating that the grafting of MMA from cellulose is controlled. The cleaved polymer brushes were compared to the concurrently formed polymer in the solution, and it was found that the surface-initiated polymerization proceeds faster than the solution polymerization at monomer conversion below 40%, but that the kinetics of the two concurrent reactions is comparable at higher conversions. At monomer conversions above 75%, the amount of termination via recombination increases, resulting in bimodal SEC traces.

The ability to tailor surface properties via ATRP from cellulose substrates has been demonstrated by the fabrication of functional bio-fiber surfaces. Superhydrophobic and self-cleaning cellulose surfaces have been produced via post-functionalization of PGMA-brushes. GMA was grafted from the surface, and the epoxide groups were utilized to create a branched "graft-on-graft" architecture of the polymer brushes. Post-functionalization with a fluoroalkyl chain yielded a surface with an extremely high water contact angle of above 170°. Interestingly, the modified cellulose substrate was also found to be self-cleaning. It was evident from AFM characterization that the surface possessed a micro-nano-binary structure, arising from a combination of the inherent roughness of the substrate and the grafting architecture. It was also found that superhydrophobic and self-cleaning cellulose surfaces with a water contact angle of around 165° could be achieved by post-functionalization with an alkyl chain, with no use of fluorine.

Stimuli-responsive bio-fiber surfaces have been achieved *via* grafting of NIPAAm and 4VP from a cellulose substrate. The PNIPAAm-grafted cellulose

surface showed hydrophilic character below the LCST, and hydrophobic above. It was found that large amounts of grafted PNIPAAm breaks up the interfibrillar structure in the cellulose substrate, resulting in increased wettability even at high temperatures. Employing a branched "graft-on-graft" architecture of the brushes by grafting NIPAAm from initiator-modified PGMA brushes, the CA above LCST could be increased by 20°. Also, the stability of the CA was increased by this method. The P4VP-grafted cellulose surfaces exhibited a pH-responsive behavior, with changes in surface wettability from hydrophilic at pH 3 to hydrophobic at pH 9. Dual-responsive bio-fiber surfaces were achieved *via* grafting of PNIPAAm-*b*-P4VP, and P4VP-*b*-PNIPAAm. The surfaces respond to changes both in temperature and pH. The length and position of the different blocks affects the surface properties, and allows further tailoring of the responsivity of the material.

6 FUTURE WORK

Surface-modification of cellulose *via* ATRP is an interesting route to bio-fibers with tailored surface properties, and further studies could increase the understanding of the field, and explore the possible applications.

The methodology for cleaving grafted polymer from a cellulose surface needs to be further investigated in terms of functional polymers, such as PGMA, which could be cleaved without affecting the functional group. Adopting the cleavage technique for other types of cellulose substrates would allow for a more detailed study on the effect of substrate differences on the graft-modification. Furthermore, by using a celluose substrate with larger surface area, such as MCC, larger amounts of polymer would be grafted and thereby facilitate the isolation of cleaved polymer.

The use of bio-fiber substrates as base for the preparation of functional surfaces is an interesting field as it could lead to new application areas for cellulose. Stimuli-responsive cellulose could be explored for the possible use in biomedical applications, such as drug delivery systems. It would be interesting to perform *in vitro* studies of protein adsorption and cell adhesion/detachment on these surfaces. Graft-modification using a combination of ATRP and ROP would allow for the synthesis of polymer brushes with bio-degradable segments combined with functional groups that could be used for conjugation of a drug or other biomedical molecules.

The use of surface-modified pulp fibers with tailored properties in papermaking or as reinforcing agents in composites is also interesting and should be explored.

7 ACKNOWLEDGEMENTS

First of all, I would like to thank my excellent supervisor Prof. Eva Malmström for the support and guidance throughout my work, for finding time for scientific discussions even at the most stressful times, and for always being so enthusiastic about the research.

I would also like to thank Prof. Anders Hult and Prof. Mats Johansson for contributing to make ytgruppen such a nice research group to work in.

All the other senior scientists at FPT are thanked for their hard work, and for creating an inspiring and creative atmosphere at the department. All members of the administrative staff are thanked for their help, especially Inger Lord for always taking the time to answer questions and helping me with the paperwork.

BiMaC (Biofibre Materials Centre) is gratefully acknowledged for financial support.

Dr. Micael Stehr and Prof. Tom Lindström are thanked for taking good care of the BiMaC students. The BiMaC students are thanked for valuable discussions, and all the good times at the field trips.

Dr. Simon Harrisson is thanked for teaching me AFM.

All the PhD students at the department are thanked for making this such a friendly place to work at. I would especially like to thank Malin E., Rikard, Sverker, Peter J. and Stefan for always taking the time to answer my cellulose-related questions.

To all the former and present members of Ytgruppen: You are like a second family to me, and I feel so lucky to have had the opportunity to share these years with you. In the last stressful weeks of writing this thesis I have become truly amazed with your kindness, helpfulness and patience. A special thanks to my co-authors who worked really late nights with me in the last week! Thanks to Emma for being a team with me and for the Paris-time in St. Louis, Danne for always saying "Of course it will work! Why wouldn't it work?" and for surviving my multi-colored 'försöksplaneringar', Linda for the emotional support and for the 13 years of working together, Anna for being an excellent lab-teacher, and for being so enthusiastic about research and Melodifestivalen, Andreas for the floors, Peter for being a peterifying room-mate, Daniel S. "the Lastbilsdoktor" for being a less space-consuming room-mate, Johan for always being so kind and helpful, Ci for preparing great food, Tommy for the unexpected return, Magnus

for being so good at getting the ducknose, George for the lunches at the "Italian place", Jarmo for not wearing shiny, neon-colored clothes, Camilla for being the 'Cam-Cam', Stor-Robban for being a really nice person behind the annoying facade, Kattis for her steady and relaxed personality, Pelle for all the laughs, and for taking the Weight-Battle Competition so seriously, Michael for returning to the group, Hanna for all the girls-talk, Neil for teaching me which tea I can put milk in, Lill-Robban for the ice-cold debating skills, and Pontus for bringing the ytgruppen-legacy into the next generation. I would also like to thank all the diploma workers and project workers who have visited the group over the years.

To my friends in the 'real world'; thank you for reminding me that there is a world outside of the lab, and for your patience with my at times very unsocial behavior during this work.

The Hoffmann family is thanked for making me feel like one of you and for trying your best to understand my weak German.

I would like to thank my whole large family, especially my sister Mikaela and my aunt, and extra sister, Susanna for always being there for me. To my parents, Marianne and Torbjörn; thank you for your unconditional love and for supporting me in everything that I decide to do. I also thank you for the domestic service during the last months of this work.

Finally to Markus; thank you for the chemistry discussions, for supporting and criticizing my work, and for surviving all the jokes about the war. And more importantly; for understanding me better than anyone else, and for showing me what love is all about. Ich liebe dich!

8 REFERENCES

(1) Georges, M. K.; Veregin, R. P. N.; Kazmaier, P. M.; Hamer, G. K. *Macromolecules* **1993**, *26*, 2987-2988.

(2) Wang, J.-S.; Matyjaszewski, K. *Macromolecules* **1995**, *28*, 7901-7910.

(3) Wang, J.-S.; Matyjaszewski, K. *J. Am. Chem. Soc.* **1995**, *117*, 5614-5615.

(4) Kato, M.; Kamigaito, M.; Sawamoto, M.; Higashimura, T. *Macromolecules* **1995**, *28*, 1721-1723.

(5) Chiefari, J.; Chong, Y. K.; Ercole, F.; Krstina, J.; Jeffery, J.; Le, T. P. T.; Mayadunne, R. T. A.; Meijs, G. F.; Moad, C. L.; Moad, G.; Rizzardo, E.; Thang, S. H. *Macromolecules* **1998**, *31*, 5559-5562.

(6) Mayadunne, R. T. A.; Rizzardo, E.; Chiefari, J.; Chong, Y. K.; Moad, G.; Thang, S. H. *Macromolecules* **1999**, *32*, 6977-6980.

(7) Kharasch, M. S.; Jensen, E. V.; Urry, W. H. *Science (Washington, DC, U. S.)* **1945**, *102*, 128.

(8) Matyjaszewski, K.; Xia, J. *Chem. Rev.* **2001**, *101*, 2921-2990.

(9) Qiu, J.; Matyjaszewski, K. *Macromolecules* **1997**, *30*, 5643-5648.

(10) Haddleton, D. M.; Jasieczek, C. B.; Hannon, M. J.; Shooter, A. J. *Macromolecules* **1997**, *30*, 2190-2193.

(11) Coca, S.; Jasieczek, C. B.; Beers, K. L.; Matyjaszewski, K. *J. Polym. Sci., Part A: Polym. Chem.* **1998**, *36*, 1417-1424.

(12) Wang, X. S.; Lascelles, S. F.; Jackson, R. A.; Armes, S. P. *Chem. Commun.* **1999**, 1817-1818.

(13) Beers, K. L.; Boo, S.; Gaynor, S. G.; Matyjaszewski, K. *Macromolecules* **1999**, *32*, 5772-5776.

(14) Davis, K. A.; Matyjaszewski, K. *Macromolecules* **2000**, *33*, 4039-4047.

(15) Krishnan, R.; Srinivasan, K. S. V. *Macromolecules* **2003**, *36*, 1769-1771.

(16) Teodorescu, M.; Matyjaszewski, K. *Macromolecules* **1999**, *32*, 4826-4831.

(17) Teodorescu, M.; Matyjaszewski, K. *Macromol. Rapid Commun.* **2000**, *21*, 190-194.

(18) Matyjaszewski, K.; Jo, S. M.; Paik, H.-j.; Gaynor, S. G. *Macromolecules* **1997**, *30*, 6398-6400.

(19) Matyjaszewski, K.; Jo, S. M.; Paik, H.-j.; Shipp, D. A. *Macromolecules* **1999**, *32*, 6431-6438.

(20) Patten, T. E.; Matyjaszewski, K. *Adv. Mater. (Weinheim, Ger.)* **1998**, *10*, 901-915.

(21) Matyjaszewski, K.; Wei, M.; Xia, J.; McDermott, N. E. *Macromolecules* **1997**, *30*, 8161-8164.
(22) Ando, T.; Kamigaito, M.; Sawamoto, M. *Macromolecules* **1997**, *30*, 4507-4510.
(23) O'Reilly, R. K.; Gibson, V. C.; White, A. J. P.; Williams, D. J. *Polyhedron* **2004**, *23*, 2921-2928.
(24) Simal, F.; Demonceau, A.; Noels, A. F. *Angew. Chem., Int. Ed.* **1999**, *38*, 538-540.
(25) Braunecker, W. A.; Itami, Y.; Matyjaszewski, K. *Macromolecules* **2005**, *38*, 9402-9404.
(26) Brandts, J. A. M.; van de Geijn, P.; van Faassen, E. E.; Boersma, J.; Van Koten, G. *J. Organomet. Chem.* **1999**, *584*, 246-253.
(27) Le Grognec, E.; Claverie, J.; Poli, R. *J. Am. Chem. Soc.* **2001**, *123*, 9513-9524.
(28) Maria, S.; Stoffelbach, F.; Mata, J.; Daran, J.-C.; Richard, P.; Poli, R. *J. Am. Chem. Soc.* **2005**, *127*, 5946-5956.
(29) Kotani, Y.; Kamigaito, M.; Sawamoto, M. *Macromolecules* **1999**, *32*, 2420-2424.
(30) Granel, C.; Dubois, P.; Jerome, R.; Teyssie, P. *Macromolecules* **1996**, *29*, 8576-8582.
(31) Uegaki, H.; Kotani, Y.; Kamigaito, M.; Sawamoto, M. *Macromolecules* **1997**, *30*, 2249-2253.
(32) Lecomte, P.; Drapier, I.; Dubois, P.; Teyssie, P.; Jerome, R. *Macromolecules* **1997**, *30*, 7631-7633.
(33) Moineau, G.; Granel, C.; Dubois, P.; Jerome, R.; Teyssie, P. *Macromolecules* **1998**, *31*, 542-544.
(34) Percec, V.; Barboiu, B.; Neumann, A.; Ronda, J. C.; Zhao, M. *Macromolecules* **1996**, *29*, 3665-3668.
(35) Wang, B.; Zhuang, Y.; Luo, X.; Xu, S.; Zhou, X. *Macromolecules* **2003**, *36*, 9684-9686.
(36) Kabachii, Y. A.; Kochev, S. Y.; Bronstein, L. M.; Blagodatskikh, I. B.; Valetsky, P. M. *Polymer Bulletin (Berlin, Germany)* **2003**, *50*, 271-278.
(37) Xia, J.; Gaynor, S. G.; Matyjaszewski, K. *Macromolecules* **1998**, *31*, 5958-5959.
(38) Xia, J.; Matyjaszewski, K. *Macromolecules* **1997**, *30*, 7697-7700.
(39) Destarac, M.; Bessiere, J. M.; Boutevin, B. *Macromol. Rapid Commun.* **1997**, *18*, 967-974.
(40) Ashford, E. J.; Naldi, V.; O'Dell, R.; Billingham, N. C.; Armes, S. P. *Chem. Commun.* **1999**, 1285-1286.
(41) Wang, X. S.; Jackson, R. A.; Armes, S. P. *Macromolecules* **2000**, *33*, 255-257.
(42) Wang, X. S.; Armes, S. P. *Macromolecules* **2000**, *33*, 6640-6647.

(43) Robinson, K. L.; Khan, M. A.; de Banez, M. V.; Wang, X. S.; Armes, S. P. *Macromolecules* **2001**, *34*, 3155-3158.
(44) Zeng, F.; Shen, Y.; Zhu, S.; Pelton, R. *J. Polym. Sci., Part A: Polym. Chem.* **2000**, *38*, 3821-3827.
(45) Perrier, S.; Armes, S. P.; Wang, X. S.; Malet, F.; Haddleton, D. M. *J. Polym. Sci., Part A: Polym. Chem.* **2001**, *39*, 1696-1707.
(46) Qiu, J.; Charleux, B.; Matyjaszewski, K. *Prog. Polym. Sci.* **2001**, *26*, 2083-2134.
(47) Tsarevsky, N. V.; Matyjaszewski, K. *J. Polym. Sci., Part A: Polym. Chem.* **2006**, *44*, 5098-5112.
(48) Shen, Y.; Tang, H.; Ding, S. *Prog. Polym. Sci.* **2004**, *29*, 1053-1078.
(49) Matyjaszewski, K.; Patten, T. E.; Xia, J. *J. Am. Chem. Soc.* **1997**, *119*, 674-680.
(50) Fischer, H. *Chem. Rev.* **2001**, *101*, 3581-3610.
(51) Wang, X.-S.; Luo, N.; Ying, S.-K. *Polymer* **1999**, *40*, 4157-4161.
(52) Harrisson, S.; Rourke, J. P.; Haddleton, D. M. *Chem. Commun.* **2002**, 1470-1471.
(53) Percec, V.; Guliashvili, T.; Ladislaw, J. S.; Wistrand, A.; Stjerndahl, A.; Sienkowska, M. J.; Monteiro, M. J.; Sahoo, S. *J. Am. Chem. Soc.* **2006**, *128*, 14156-14165.
(54) Milner, S. T. *Science (Washington, DC, U. S.)* **1991**, *251*, 905-914.
(55) Zhao, B.; Brittain, W. J. *Prog. Polym. Sci.* **2000**, *25*, 677-710.
(56) Ejaz, M.; Yamamoto, S.; Ohno, K.; Tsujii, Y.; Fukuda, T. *Macromolecules* **1998**, *31*, 5934-5936.
(57) Husseman, M.; Malmström, E. E.; McNamara, M.; Mate, M.; Mecerreyes, D.; Benoit, D. G.; Hedrick, J. L.; Mansky, P.; Huang, E.; Russell, T. P.; Hawker, C. J. *Macromolecules* **1999**, *32*, 1424-1431.
(58) Zhao, B.; Brittain, W. J. *J. Am. Chem. Soc.* **1999**, *121*, 3557-3558.
(59) Matyjaszewski, K.; Miller, P. J.; Shukla, N.; Immaraporn, B.; Gelman, A.; Luokala, B. B.; Siclovan, T. M.; Kickelbick, G.; Vallant, T.; Hoffmann, H.; Pakula, T. *Macromolecules* **1999**, *32*, 8716-8724.
(60) Kim, J.-B.; Bruening, M. L.; Baker, G. L. *J. Am. Chem. Soc.* **2000**, *122*, 7616-7617.
(61) Shah, R. R.; Merreceyes, D.; Husemann, M.; Rees, I.; Abbott, N. L.; Hawker, C. J.; Hedrick, J. L. *Macromolecules* **2000**, *33*, 597-605.
(62) Von Werne, T.; Patten, T. E. *J. Am. Chem. Soc.* **1999**, *121*, 7409-7410.
(63) Liu, T.; Casado-Portilla, R.; Belmont, J.; Matyjaszewski, K. *J. Polym. Sci., Part A: Polym. Chem.* **2005**, *43*, 4695-4709.
(64) Carlmark, A.; Malmström, E. *J. Am. Chem. Soc.* **2002**, *124*, 900-901.

(65) Angot, S.; Ayres, N.; Bon, S. A. F.; Haddleton, D. M. *Macromolecules* **2001**, *34*, 768-774.
(66) Pyun, J.; Kowalewski, T.; Matyjaszewski, K. *Macromol. Rapid Commun.* **2003**, *24*, 1043-1059.
(67) Prucker, O.; Ruehe, J. *Langmuir* **1998**, *14*, 6893-6898.
(68) Ejaz, M.; Tsujii, Y.; Fukuda, T. *Polymer* **2001**, *42*, 6811-6815.
(69) Ohno, K.; Morinaga, T.; Koh, K.; Tsujii, Y.; Fukuda, T. *Macromolecules* **2005**, *38*, 2137-2142.
(70) Fournier, D.; Pascual, S.; Montembault, V.; Haddleton, D. M.; Fontaine, L. *J. Comb. Chem.* **2006**, *8*, 522-530.
(71) Sun, T.; Wang, G.; Feng, L.; Liu, B.; Ma, Y.; Jiang, L.; Zhu, D. *Angew. Chem., Int. Ed.* **2004**, *43*, 357-360.
(72) Zhai, G.; Shi Zhi, L.; Kang En, T.; Neoh Koon, G. *Macromol Biosci FIELD Full Journal Title:Macromolecular bioscience* **2005**, *5*, 974-982.
(73) Ma, H.; Hyun, J.; Stiller, P.; Chilkoti, A. *Adv. Mater. (Weinheim, Ger.)* **2004**, *16*, 338-341.
(74) Xu, F. J.; Zhong, S. P.; Yung, L. Y. L.; Kang, E. T.; Neoh, K. G. *Biomacromolecules* **2004**, *5*, 2392-2403.
(75) Zhou, F.; Huck, W. T. S. *Phys. Chem. Chem. Phys.* **2006**, *8*, 3815-3823.
(76) Galaev, I. Y.; Mattiasson, B. *Trends Biotechnol.* **1999**, *17*, 335-340.
(77) Gould, P. *Materials Today (Oxford, United Kingdom)* **2003**, *6*, 44-48.
(78) Nakajima, A.; Hashimoto, K.; Watanabe, T. *Monatsh. Chem.* **2001**, *132*, 31-41.
(79) Blossey, R. *Nat. Mater.* **2003**, *2*, 301-306.
(80) Callies, M.; Quere, D. *Soft Matter* **2005**, *1*, 55-61.
(81) Wenzel, R. N. *Journal of Industrial and Engineering Chemistry (Washington, D. C.)* **1936**, *28*, 988-994.
(82) Cassie, A. B. D.; Baxter, S. *Trans. Faraday Soc.* **1944**, *40*, 546-551.
(83) Murase, H.; Fujibayashi, T. *Prog. Org. Coat.* **1997**, *31*, 97-104.
(84) Miwa, M.; Nakajima, A.; Fujishima, A.; Hashimoto, K.; Watanabe, T. *Langmuir* **2000**, *16*, 5754-5760.
(85) Barthlott, W.; Neinhuis, C. *Planta* **1997**, *202*, 1-8.
(86) Xie, Q.; Fan, G.; Zhao, N.; Guo, X.; Xu, J.; Dong, J.; Zhang, L.; Zhang, Y.; Han, C. C. *Adv. Mater. (Weinheim, Ger.)* **2004**, *16*, 1830-1833.
(87) Guo, Z.; Zhou, F.; Hao, J.; Liu, W. *J. Am. Chem. Soc.* **2005**, *127*, 15670-15671.
(88) Han, J. T.; Lee, D. H.; Ryu, C. Y.; Cho, K. *J. Am. Chem. Soc.* **2004**, *126*, 4796-4797.
(89) Yamanaka, M.; Sada, K.; Miyata, M.; Hanabusa, K.; Nakano, K. *Chem. Commun.* **2006**, 2248-2250.

(90) Roig, A.; Molins, E.; Rodriguez, E.; Martinez, S.; Moreno-Manas, M.; Vallribera, A. *Chem. Commun.* **2004**, 2316-2317.
(91) Shirtcliffe, N. J.; McHale, G.; Newton, M. I.; Perry, C. C.; Roach, P. *Chem. Commun.* **2005**, 3135-3137.
(92) Gu, Z.-Z.; Uetsuka, H.; Takahashi, K.; Nakajima, R.; Onishi, H.; Fujishima, A.; Sato, O. *Angew. Chem., Int. Ed.* **2003**, *42*, 894-897.
(93) Zhang, G.; Wang, D.; Gu, Z.-Z.; Moehwald, H. *Langmuir* **2005**, *21*, 9143-9148.
(94) Russell, T. P. *Science (Washington, DC, U. S.)* **2002**, *297*, 964-967.
(95) Luzinov, I.; Minko, S.; Tsukruk, V. V. *Prog. Polym. Sci.* **2004**, *29*, 635-698.
(96) Nath, N.; Chilkoti, A. *Adv. Mater. (Weinheim, Ger.)* **2002**, *14*, 1243-1247.
(97) Schild, H. G. *Prog. Polym. Sci.* **1992**, *17*, 163-249.
(98) Heskins, M.; Guillet, J. E. *Journal of Macromolecular Science, Chemistry* **1968**, *2*, 1441-1455.
(99) Lin, S.-Y.; Chen, K.-S.; Run-Chu, L. *Polymer* **1999**, *40*, 2619-2624.
(100) Takei, Y. G.; Aoki, T.; Sanui, K.; Ogata, N.; Sakurai, Y.; Okano, T. *Macromolecules* **1994**, *27*, 6163-6166.
(101) Fu, Q.; Rao, G. V. R.; Basame, S. B.; Keller, D. J.; Artyushkova, K.; Fulghum, J. E.; Lopez, G. P. *J. Am. Chem. Soc.* **2004**, *126*, 8904-8905.
(102) Pu, H.; Ding, Z.; Ma, Z. *J. Appl. Polym. Sci.* **1996**, *62*, 1529-1535.
(103) Liang, L.; Feng, X.; Liu, J.; Rieke, P. C.; Fryxell, G. E. *Macromolecules* **1998**, *31*, 7845-7850.
(104) Huber, D. L.; Manginell, R. P.; Samara, M. A.; Kim, B.-I.; Bunker, B. C. *Science (Washington, DC, U. S.)* **2003**, *301*, 352-354.
(105) Balamurugan, S.; Mendez, S.; Balamurugan, S. S.; O'Brien, M. J.; Lopez, G. P. *Langmuir* **2003**, *19*, 2545-2549.
(106) Kim, D. J.; Heo, J.-y.; Kim, K. S.; Choi, I. S. *Macromol. Rapid Commun.* **2003**, *24*, 517-521.
(107) Kim, D. J.; Kang, S. M.; Kong, B.; Kim, W.-J.; Paik, H.-j.; Choi, H.; Choi, I. S. *Macromol. Chem. Phys.* **2005**, *206*, 1941-1946.
(108) Schmaljohann, D.; Oswald, J.; Jorgensen, B.; Nitschke, M.; Beyerlein, D.; Werner, C. *Biomacromolecules* **2003**, *4*, 1733-1739.
(109) Akiyama, Y.; Kikuchi, A.; Yamato, M.; Okano, T. *Langmuir* **2004**, *20*, 5506-5511.
(110) Xu, F. J.; Zhong, S. P.; Yung, L. Y. L.; Tong, Y. W.; Kang, E.-T.; Neoh, K. G. *Biomaterials* **2006**, *27*, 1236-1245.
(111) Iwata, H.; Hirata, I.; Ikada, Y. *Langmuir* **1997**, *13*, 3063-3066.
(112) Shen, H.; Zhang, L.; Eisenberg, A. *J. Am. Chem. Soc.* **1999**, *121*, 2728-2740.
(113) Ayres, N.; Cyrus, C. D.; Brittain, W. J. *Langmuir*, ACS ASAP.

(114) Xia, F.; Feng, L.; Wang, S.; Sun, T.; Song, W.; Jiang, W.; Jiang, L. *Adv. Mater. (Weinheim, Ger.)* **2006**, *18*, 432-436.
(115) Klemm, D.; Heublein, B.; Fink, H.-P.; Bohn, A. *Angew. Chem., Int. Ed.* **2005**, *44*, 3358-3393.
(116) Gardner, K. H.; Blackwell, J. *Biopolymers* **1974**, *13*, 1975-2001.
(117) Krässig, H. A. *Cellulose-Structure, Accessibility, and Reactivity*; Gordon and Breach: Amsterdam, 1993.
(118) Hebeish, A.; Guthrie, J. T. *Polymers, Vol. 4: The Chemistry and Technology of Cellulosic Copolymers*; Springer-Verlag, Berlin, Fed. Rep. Ger., 1981; Vol. 4.
(119) Cruz-Ramos, C. A. In *Mechanical Properties of Reinforced Thermoplastics*; Clegg, D. W.; Collyer, A. A., Eds.; Elsevier Applied Science Publishers: London and New York, 1986.
(120) Joly, C.; Gauthier, R.; Chabert, B. *Composites Science and Technology* **1996**, *56*, 761-765.
(121) Immergut, E. H.; Mark, H. *Makromol. Chem.* **1956**, *18/19*, 322-341.
(122) Mino, G.; Kaizerman, S. *Journal of Polymer Science* **1958**, *31*, 242-243.
(123) Geacintov, N.; Stannett, V.; Abrahamson, E. W.; Hermans, J. J. *J. Appl. Polym. Sci.* **1960**, *3*, 54-60.
(124) Schwab, E.; Stannett, V.; Hermans, J. J. *Tappi* **1961**, *44*, 251-256.
(125) Yasuda, I. H.; Wray, J. A.; Stannett, V. *Journal of Polymer Science* **1963**, *Pt. C*, 387-402.
(126) Chaudhuri, D. K. R.; Hermans, J. J. *Journal of Polymer Science* **1960**, *48*, 159-166.
(127) Chaudhuri, D. K. R.; Hermans, J. J. *Journal of Polymer Science* **1961**, *51*, 373-381.
(128) Hatakeyama, H.; Rånby, B. *Cellul. Chem. Technol.* **1975**, *9*, 583-596.
(129) Rånby, B.; Rodehed, C. *ACS Symp. Ser.* **1981**, *175*, 253-264.
(130) Rånby, B.; Zuchowska, D. *Polym. J. (Tokyo, Jpn.)* **1987**, *19*, 623-630.
(131) Gurdag, G.; Guclu, G.; Ozgumus, S. *J. Appl. Polym. Sci.* **2001**, *80*, 2267-2272.
(132) Gupta, K. C.; Sahoo, S. *Biomacromolecules* **2001**, *2*, 239-247.
(133) Biermann, C. J.; Chung, J. B.; Narayan, R. *Macromolecules* **1987**, *20*, 954-957.
(134) Månsson, P.; Westfeldt, L. *Journal of Polymer Science: Polymer Chemistry Edition* **1981**, *19*, 1509-1515.
(135) Tsubokawa, N.; Iida, T.; Takayama, T. *J. Appl. Polym. Sci.* **2000**, *75*, 515-522.
(136) Daly, W. H.; Evenson, T. S.; Iacono, S. T.; Jones, R. W. *Macromol. Symp.* **2001**, *174*, 155-163.
(137) Roy, D.; Guthrie, J. T.; Perrier, S. *Macromolecules* **2005**, *38*, 10363-10372.

(138) Carlmark, A.; Malmström, E. E. *Biomacromolecules* **2003**, *4*, 1740-1745.
(139) Lee, S. B.; Koepsel, R. R.; Morley, S. W.; Matyjaszewski, K.; Sun, Y.; Russell, A. J. *Biomacromolecules* **2004**, *5*, 877-882.
(140) Ciampolini, M.; Nardi, N. *Inorg. Chem.* **1966**, *5*, 41-44.
(141) Plackett, D.; Jankova, K.; Egsgaard, H.; Hvilsted, S. *Biomacromolecules* **2005**, *6*, 2474-2484.
(142) Franz, R.; Fritsche-Lang, W.; Deger, H. M.; Erckel, R.; Schlingmann, M. *J. Appl. Polym. Sci.* **1987**, *33*, 1291-1306.
(143) Xia, J.; Zhang, X.; Matyjaszewski, K. *Macromolecules* **1999**, *32*, 3531-3533.
(144) Tsarevsky, N. V.; Braunecker, W. A.; Brooks, S. J.; Matyjaszewski, K. *Macromolecules* **2006**, *39*, 6817-6824.
(145) Ruokolainen, J.; ten Brinke, G.; Ikkala, O.; Torkkeli, M.; Serimaa, R. *Macromolecules* **1996**, *29*, 3409-3415.
(146) Li, D.; He, Q.; Cui, Y.; Li, J. *Chem. Mater.* **2007**, *19*, 412-417.